Journal of Polymer Science and Engineering (2023) Volume 6 Issue 1
doi: 10.24294/jpse.v6i1.3292

REVIEW ARTICLE

High-performance functional materials based on polymer nanocomposites—A review

Mohan Raj Krishnan*, Edreese Housni Alsharaeh*

College of Science and General Studies, AlFaisal University, PO Box 50927, Riyadh 11533, Saudi Arabia

*** Corresponding authors**: Mohan Raj Krishnan, mkrishnan@alfaisal.edu;
Edreese Housni Alsharaeh, ealsharaeh@alfaisal.edu

ABSTRACT

Oil spill clean-up is a long-standing challenge for researchers to prevent serious environmental pollution. A new kind of oil-absorbent based on silicon-containing polymers (e.g., poly(dimethylsiloxane) (PDMS)) with high absorption capacity and excellent reusability was prepared and used for oil-water separation. The PDMS-based oil absorbents have highly interconnected pores with swellable skeletons, combining the advantages of porous materials and gels. On the other hand, polymer/silica composites have been extensively studied as high-performance functional coatings since, as an organic/inorganic composite material, they are expected to combine polymer flexibility and ease of processing with mechanical properties. Polymer composites with increased impact resistance and tensile strength without decreasing the flexibility of the polymer matrix can be achieved by incorporating silica nanoparticles, nanosand, or sand particles into the polymeric matrices. Therefore, polymer/silica composites have attracted great interest in many industries. Some potential applications, including high-performance coatings, electronics and optical applications, membranes, sensors, materials for metal uptake, etc., were comprehensively reviewed. In the first part of the review, we will cover the recent progress of oil absorbents based on silicon-containing polymers (PDMS). In the later details of the review, we will discuss the recent developments of functional materials based on polymer/silica composites, sand, and nanosand systems.

Keywords: polymer; oil-spill; porous materials; composites; silica; nanoparticles

ARTICLE INFO

Received: 5 November 2023
Accepted: 8 December 2023
Available online: 22 December 2023

1. Introduction

Various industries, such as mining and petrochemicals, produce enormous volumes of oily water, which has become a ubiquitous pollutant worldwide and is now considered a serious global environmental concern[1]. For instance, a typical mining operation produces approximately 140,000 L of oil-contaminated water daily[2]. In addition, the frequent oil leakages/spillages during marine transportation or oil production are a potential catastrophe to marine environments and ecology and a tremendous waste of valuable natural resources. Various oil/water separation methods and novel materials have been reported to address these issues[3]. The oil-water separation technologies using multiple types of materials are summarized in **Figure 1**.

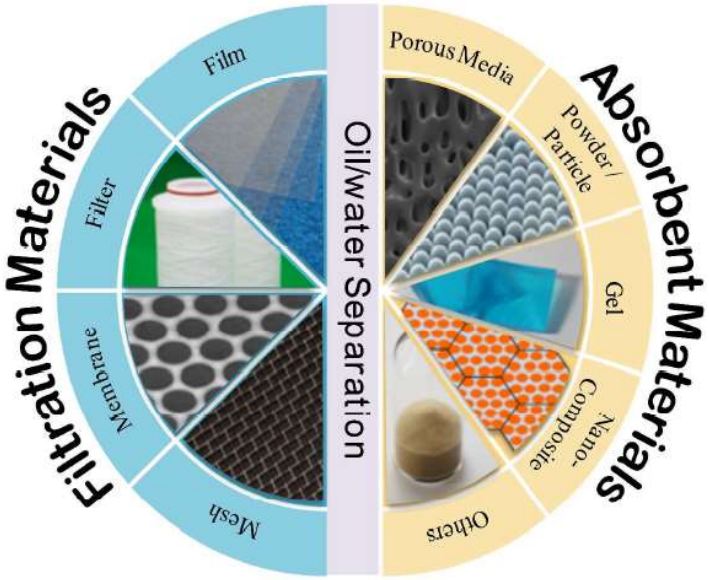

Figure 1. The summary of the recent progress of oil/water separation technologies using various materials[3]. Reproduced with permission from the Royal Society of Chemistry.

Among the various developed technologies for oil and organic solvent clean-up, the absorption technique has excellent advantages in terms of operational simplicity, cost-effectiveness, and complete clean-up without any secondary pollution[4,5]. At present, the oil absorbents are classified into three major categories: (a) porous materials; (b) self-assembled fibers and gels[6–11]. Among them, porous materials and polymers with interconnected network structures and swelling properties with considerable high hydrophobicity and oleophilicity are found to be potential candidates for oil absorption due to their outstanding oil selectivity, very high absorption capacities, fast kinetics, excellent material reusability, and enhanced oil recovery[12–18]. Recently, PDMS-based absorbents were found to be a potential candidate for oil absorption due to their high hydrophobicity, oleophilicity, and commercial availability[19]. In addition, the PDMS has been used to selectively separate oils and/or organic solvents from water selectively[20]. The PDMS has been the most widely used silicon-based organic elastomer since Wacker Chemie synthesized the first silicones in the 1950s and its introduction to academic laboratories in the 1990s[21,22]. PDMS is generally a viscoelastic, biocompatible, chemically and mechanically robust material with a low glass transition temperature, cost-effectiveness, and good moldability, ensuring it is acceptable for practical uses[23,24]. The Si-O-Si backbone endows PDMS elastomers with intriguing properties, such as high flexibility, non-toxicity, non-flammability, thermal and electrical resistance, and low bulk density[25]. PDMS exhibits high transmittance and low absorption under UV irradiation and is suitable for desirable optical applications[26]. Because of its excellent contour accuracy of less than 10 nm, PDMS is widely exploited in micro- and nanotechnologies[22,27]. Solid PDMS is resistant to most aqueous reagents and alcohol solvents. However, organic solvents such as xylene can swell this elastomer[28]. Meanwhile, it is permeable to small, unreactive vapor and gas molecules such as water and oxygen[29,30]. Moreover, the surface of pristine PDMS presents low surface tension and energy and is hydrophobic. The wettability can be changed to hydrophilic temporarily by massively introducing hydroxyl groups with oxygen plasma treatment, yet it regains its hydrophobic property due to chain migration[31]. The PDMS surface can be easily modified via plasma oxygenation, adsorption of proteins, or conjugation of other functional chemical groups[32,33]. The high electronegativity can also be utilized to deposit oppositely charged electrolytes for hydrophilic modification and to realize extensive electrical applications[34].

PDMS sponges, as one of the most important porous polymeric materials, involve quite a broad subject in relation to their chemical and physical structures, fabrication techniques, optimized properties, and desired applications[35]. To date, several excellent reviews on the development of porous polymeric materials have been published in the most recent years[25,36–43]. Readers can consult the comprehensive reviews to understand

structure design, synthesis strategies, correlated functions, and applications. However, PDMS sponges have been rarely mentioned in these existing reviews. Considering their outstanding properties and growing research interest, we believe that offering a focused review to summarize these newly emerged design strategies and applications is very important for developing elastic PDMS sponges.

On the other hand, the silica/polymer composite materials combine the rigidity and high thermal stability of the inorganic component with the organic polymer component's flexibility, ductility, and processability[44–51]. The silica nanoparticles have many interesting properties, including high mechanical strength, permeability, thermal and chemical stability, a relatively low refractive index, and a high surface area. Incorporating the nanoparticles into polymer matrices would considerably enhance their mechanical and thermal properties and improve their insulation properties. **Figure 2** shows the schematic illustration of silica/polymer composite fabrication. Therefore, polymer/silica composite materials can exhibit various unique properties, such as optical transparency, specific electrical and mechanical characteristics, thermal and weathering resistance, abrasion resistance, and impact resistance, for high-performance coating applications. Many other applications of silica/polymer composites include metal uptake[52–58], sensors[59–62], electronics and optical materials[63–65], photoresist materials[66–68], optical devices[69–71], flame-retardant materials[72,73], proton exchange membranes[74–78], anticorrosion materials[79,80], grouting materials[81,82], oil adsorbents[83,84], biomedical materials[85–88], other coatings[89–91], etc.

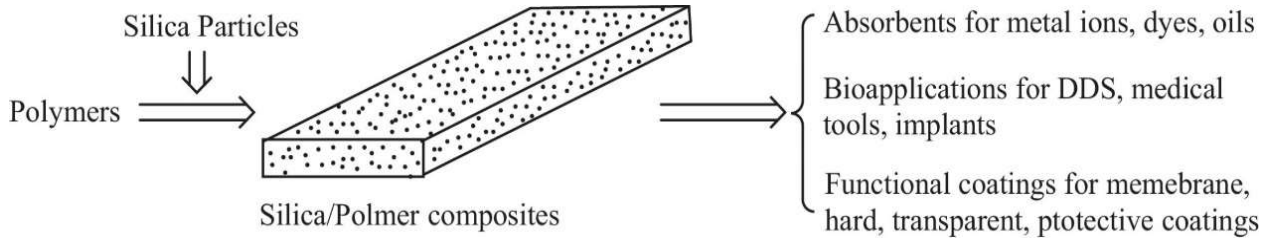

Figure 2. The schematic illustration of silica/polymer composites fabrication and its potential applications[92]. Reproduced with permission from Elsevier.

2. Oil-absorbents based on silicon-containing polymers

Therefore, it is evident that the PDMS is a widely studied system for oil-absorption applications among various silicon-containing polymers[12,93]. A straightforward and often utilized method for fabricating PDMS sponges is to use diverse solid templates, such as porogen, which can be selectively dissolved or removed to leave a PDMS skeleton with interconnected cavities. Based on the type of templates, this class of direct templating can be categorized into two main approaches using sacrificial templates, including salt crystals, sugar cubes, zinc oxide powders, nickel foam, and easily dissoluble polymer particles[94–99]. Among them all, the particulate leaching of salt or sugar cubes is the most prominent. A reason for its widespread use lies in the facile realization that no sophisticated laboratory equipment or hazardous solvent is required. In particular, water is utilized for leaching, and the leached salt or sugar particles/cubes can be retrieved afterward. Also, sugar leaching techniques are ready for scale-up production. For example, Wang et al. fabricated a bigger PDMS sponge by simply using sugar particles, which weathered a humidity of 85%[100]. The high humidity resulted in a fusion of the sugar particles, which ultimately yielded well-interconnected macroporous PDMS sponges.

Porous PDMS materials can be prepared using sugar, salt, self-assembled colloidal microspheres, emulsion droplets, and CO_2 gas generated by $NaHCO_3$ as templates, among which the sacrificial sugar template technique has been the most popular one because of its low cost and eco-friendliness[101–103]. **Figure 3** shows the schematic illustration of PDMS oil-absorbent preparation by template syntheses using various templates.

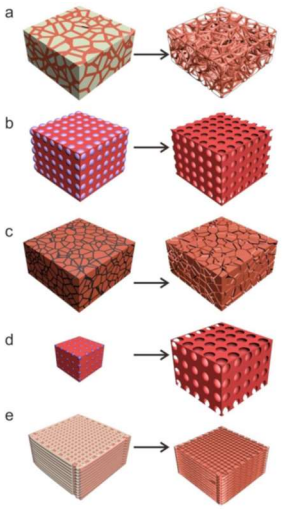

Figure 3. The schematic illustration of preparing PDMS oil absorbents using templated syntheses. **(a)** sugar cubes; **(b)** polystyrene beads; **(c)** Ni foam; **(d)** gas foaming; and **(e)** printed (3D-) templates[12]. Reproduced with permission from the Royal Society of Chemistry.

Figure 4(a) shows a typical sugar cube-leaching method for fabricating PDMS sponges[104]. Briefly, sugar cubes as the sacrificial template, are placed in a container ready for molding PDMS elastomers. Subsequently, a mixture of PDMS pre-polymer and curing agent (10:1 by weight) is poured into a pool to submerge the sugar cubes, followed by degassing in a vacuum chamber to assist the infiltration of liquid pre-polymer into the voids of the sugar cubes. Afterward, the PDMS-sugar cube is cured in an oven. Finally, the cured PDMS-sugar cubes are cut to reveal the sugar template, and the sugar portion is leached out by the water, resulting in 3D interconnected porous structures of PDMS sponges. Not limited to sugar cubes, Choi et al.[95] reported the fabrication of PDMS sponges with optimized performance in oil absorption by using sugar particles with different sizes, as shown in **Figure 4(b)**. Zhang et al.[13] reported a modified sugar leaching method by directly curing PDMS pre-polymer in a p-xylene solution in the presence of sugar particles, as shown in **Figure 4(c)**. As such, the as-made PDMS sponges have 3D interconnected pores and a swellable skeleton (**Figures 4(g)–(k)**).

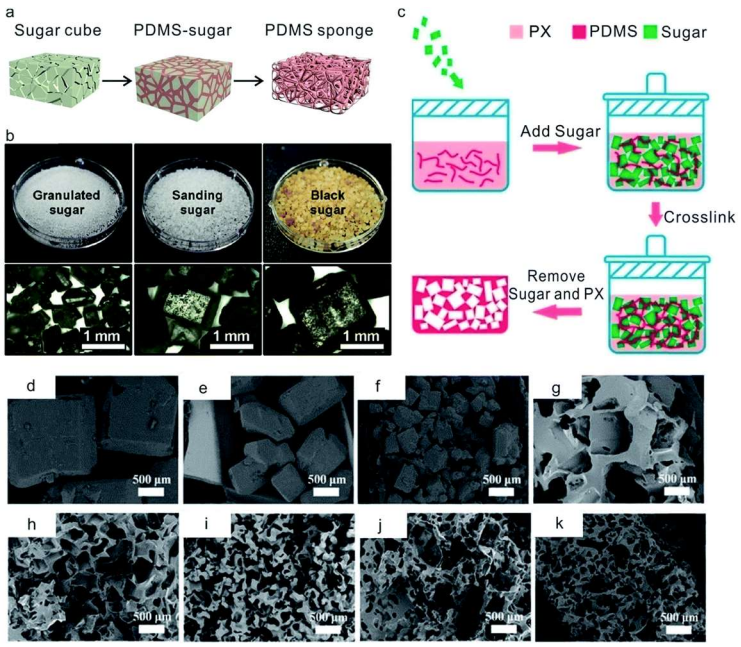

Figure 4. PDMS sponges fabricated by the sugar leaching method: **(a)** Schematic illustration of the fabrication process using a sugar cube as the template. **(b)** Photographs of sugar particles of different sizes. **(c)** A vacuum-free sugar-particle leaching method in a *p*-xylene (PX) solution, where the sugar and PX were removed after curing. **(d)–(k)** Scanning electron microscopy (SEM) images of sugar particles **(d)–(f)** and the as-made PDMS sponges **(g)–(k)**[12]. Reproduced with permission from the Royal Society of Chemistry.

PDMS sponges were also synthesized based on emulsion templates *via* the polymerization of the continuous phase of an emulsion, in which the emulsion droplets act as templates for pore formation[105–108]. The phase separation technique is promising for fabricating porous polymer membranes and 3D structures[109,110]. Jung et al.[105] systematically investigated the formation of pores during the fabrication process of a PDMS sponge and evaluated the performance of a homemade pressure sensor based on a PDMS sponge. Advances in the manufacture of additives have drawn much attention this century and have resulted in numerous improved approaches for 3D printing using PDMS[111–113]. However, the direct 3D printing of PDMS to form complex structures is still challenging, owing to the low elastic modulus of the liquid pre-polymer.

The oil and various organic solvent absorbencies of the PDMS sponge replicated from sugar templates were investigated in detail by Choi et al.[95]. The PDMS sponge was dipped into the organic solvents and oils for a few seconds. The oil-filled PDMS sponge could float on water without water penetration into the structure or the release of the oil; this was verified from the measured weight of the oil-soaked PDMS sponge, which changed by only 6% after 24 h (**Figure 5**). One important observation was that the absorbed oil was almost completely retained after the PDMS sponge was removed from the water, as evidenced by its weight remaining within 93% of the wet weight after 24 h. The PDMS sponge showed absorption capacities ranging from 400 wt% to 1100 wt% for various oils and organic solvents, with the maximum absorption capacity reaching up to 10 times its weight. The changes in absorption capacity depend on the density of the organic solvents and oils. Furthermore, the PDMS sponge also showed a high absorption capacity for nonpolar and polar organic solvents. For instance, the absorption capacity of 1,2-dichlorobenzene (a well-known toxic organic contaminant in water treatment) for the PDMS sponge based on the template with granulated and black sugar particles was approximately 1000 wt%. Because the PDMS materials show relatively excellent chemical inertness, the PDMS sponge may be used for nonpolar and polar organic solvents, with great potential for removing toxic organic contaminants and oil spills from water. Swelling of the PDMS sponge was occasionally observed along with the absorption of organic solvents because the organic solvents can diffuse into the PDMS material. Nevertheless, this swelling did not influence the sponge's absorption properties.

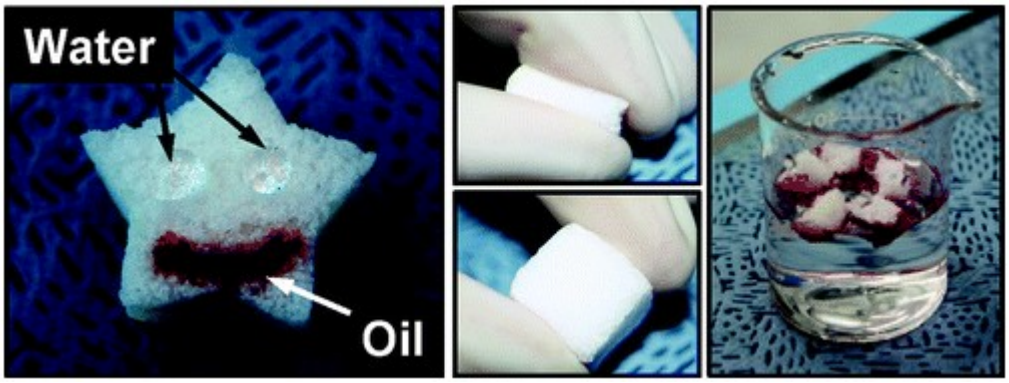

Figure 5. PDMS sponge prepared using the sugar template method for selective oil absorption from oil/water mixture[95]. Reproduced with permission from ACS.

The recyclability of the PDMS sponge and the recoverability of oils and organic solvents address critical requirements in practical oil clean-up applications. The absorbed oils and organic solvents in the PDMS sponge can be removed and reused by manually squeezing the PDMS sponge due to the springy nature of the PDMS material. As such, the fabricated PDMS sponge is desirable because it facilitates the recycling of oil-absorbent materials by allowing for the repeated capture and release of oils and organic solvents. To test the recyclability of the PDMS sponge as an absorbent material, the PDMS sponge can be squeezed and immediately immersed in an organic solvent (e.g., ethanol) 20 times after absorbing the transformer oil; the sponge weight was measured before and after drying. The reason for immersing the oil-absorbed PDMS sponge in ethanol was to ensure that any oil remaining after squeezing the oil-soaked PDMS sponge would be completely exuded into

the ethanol. The results show that the absorption capacity did not deteriorate, and the weight of a dry PDMS sponge did not notably change when the PDMS sponge was reused multiple times. When the PDMS sponge was immersed in water after the reusability test, it absorbed no water, indicating that hydrophobicity was not lost[95].

Guo et al.[114] successfully synthesized a PDMS sponge by polymerizing the pre-polymer and a curing agent in a saturated $NaHCO_3$ solution in the presence of carbon tetrachloride and n-octane (**Figure 6(a)**). Compared with the previous research, the PDMS sponges fabricated via simple and time-saving methods show excellent hydrophobicity/oleophilicity and thermal properties. The absorption capacities of the 3D interconnected porous PDMS sponges with swellable skeletons are 694%–2513% for various oils and solvents (**Figure 6(b)**). Due to their special wettability, the PDMS sponges can absorb oils and organic solvents from the oil-water mixture, and the whole separation process can be finished within 20 s. Furthermore, the oil absorption capacity of the PDMS sponge has no difference after 20 cycles and without weight loss (**Figure 6(c)**). Because of these excellent properties and simplicity of fabrication, it can be envisaged that the PDMS sponge will be a very promising material for handling oily wastewater.

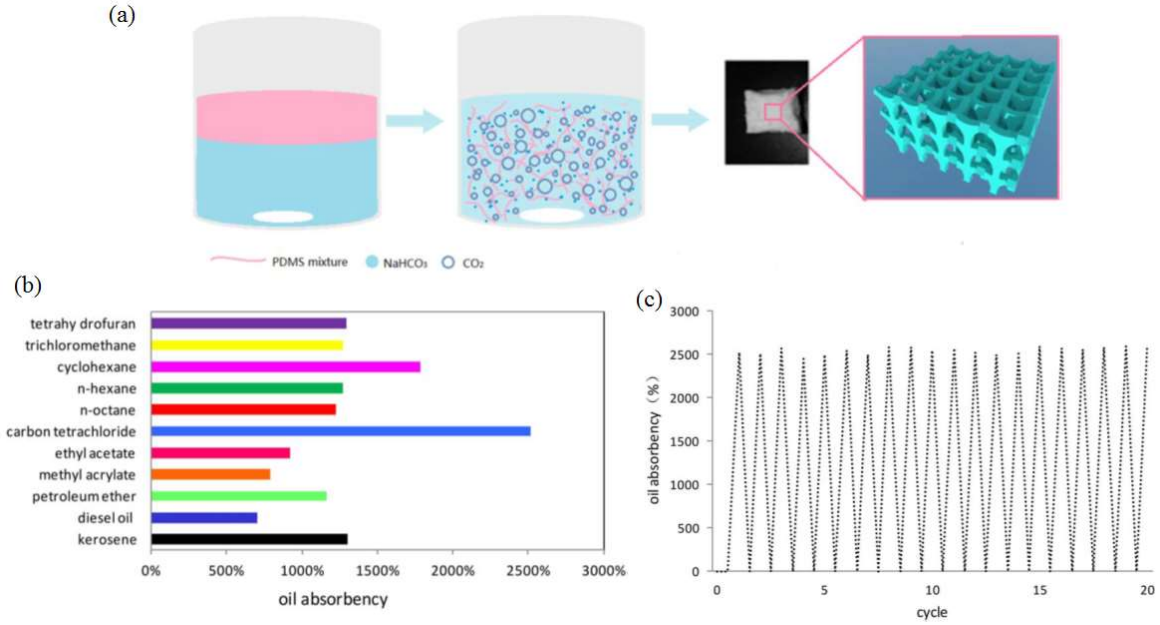

Figure 6. (a) Preparation process of PDMS oil-absorbent; **(b)** oil and organic solvents absorbency by the PDMS sponge; and **(c)** the recyclability of the absorbent. Reproduced with permission from John Wiley & Sons. Inc.[114].

Compared with the fabrication of oil-absorbents, PDMS oil-absorbents have been easily prepared and have much more stability and practical applicability. Moreover, the preparation process involves the shape of sugar templates and the necessity of a vacuum operation, inducing penetration of PDMS pre-polymer into the templates. From the viewpoint of absorption mechanism, porous absorption materials store oils and organic solvents in pores, while gels retain them among the 3D cross-linked network of molecular chains or aggregates. Therefore, the higher the porosity, the larger the absorption capacity for porous absorbents[115]. However, considering the flexibility of the PDMS molecular chain, it is only possible to increase the porosity of PDMS with a limit. High porosity may result in a collapse of the porous structure[116]. These PDMS oil absorbents have interconnected pores and swellable skeletons, which can absorb and retain oils. The high oil absorption capacity of the PDMS sponge mainly ascribes to similar surface energies between oils (e.g., ethyl acetate, 26.29 mNm^{-1}) and PDMS (20.4 mNm^{-1}). The sponge's surface strongly repels water due to a much higher surface tension (72 mNm^{-1}) than the PDMS. The capillary flow further improved the absorption capacity due to the interconnected pores of the PDMS sponge. After determining the weight of the water before and after separation, the separation efficiency is 97.9%. Compared with other sponges, PDMS sponges have excellent

advantages such as low cost, simple fabrication, good absorption capacity, and high separation efficiency[94,101,117]. The oil and organic solvent absorption capacities of various silicon-containing polymers have been summarized in **Table 1.** In addition to PDMS sponges, porous silicones have advantages when used for oil/water separation due to their high hydrophobicity, flexibility, thermal stability, and low costs[118–120]. Various porous silicones with high oil/water separation efficiency have been successfully synthesized[120,121]. For example, Moitra et al.[121] prepared porous hydrogen silsesquioxane monoliths by the sol–gel transition of trimethoxysilane, accompanied by a phase separation process.

Table 1. Summary of absorption capacities of various silicon-containing polymers.

Absorbent material	Types of oil	Absorption capacity (g/g)	References
PDMS sponge	Various oils	4.72–20	[94]
PDMS sponge	Various oils	7.90–40	[122]
PDMS sponge	Various oils	6.9–25.2	[114]
Porous PDMS	CCl_4	5.72	[117]
PU/CNT/PDMS sponge	n-Hexane	15	[123]
PU/PTFE/SiO_2/polysiloxane sponge	Silicon oil	9.9	[124]

3. Polymer/silica composites as high-performance functional materials

In recent times, scientists have paid attention to a new type of coating: organic/inorganic composite coatings[125–132]. These coatings combine the flexibility and easy processing of polymers with the hardness of inorganic materials and have been successfully applied to various substrates[133–137]. These composite coatings are generally transparent, show good adhesion, and enhance a polymeric substrate's scratch and abrasion resistance[136,138–145]. The reinforcement of acrylates by surface-modified nanosilica led to acrylate nanocomposite coatings with improved scratch and abrasion resistance[146]. These coatings can be used on substrates such as polymer films, paper, metal, wood, and engineered wood. In addition, compared with nanocomposite materials, much better abrasion resistance was obtained for coatings containing both silica nanoparticles and corundum microparticles. These nano- and micro-composites are recommended as clear coats for parquet and flooring applications. It was shown that polymer/silica nanocomposites can be obtained in various structures and compositions by using miniemulsion polymerization[147–150]. The resulting structures are possibly interesting for generating waterborne coatings, which show the polymer's ability for spontaneous film formation in combination with the high mechanical scratch resistance provided by the inorganic nanoparticles.

The simplest method for preparing polymer/silica composites is directly mixing the silica and the polymer. The mixing can generally be carried out by melt blending, solution blending, and in situ polymerization (**Figure 7**). In such mixing processes, the primary key point is the effective dispersion of the silica nanoparticles into the polymer matrix because they generally tend to agglomerate. Melt blending is most commonly utilized because of its effective processability[151]. This method has some advantages, such as being simple, cost-effective, easy to process, and widely applicable. Using a twin screw extruder and injection molding machine, the mechanical property of polymer composites loaded with nanoparticles could be better than that of a conventional compounding route in which the nanoparticles were pre-grafted by some polymers through irradiation. Melt blending for the composite of silica and the polymers is generally carried out above the polymer's glass-transition temperature (T_g). This mixing route is more efficient and operable than mechanically simple mixing at room temperature. This method is a polymer-inorganic powder blending process using a solvent in which the polymer is soluble. This processing is widely used for common composite preparation. In the dispersion of silica fillers into a polymer matrix, solution blending is much more effective

than melt blending[152]. This method can make nanofillers dispersible effectively into the polymer chains. With solvent removal, a well-dispersed silica/polymer composite can be obtained. However, there are drawbacks to the use of environmentally unfriendly organic solvents, including the selection of an appropriate solvent and the removal process of the solvent after composition, even though it can overcome the limitation of melt blending, which is not feasible due to severe shear heating and the formation of particle aggregates[45]. Polymer/mesoporous silica composites were commonly carried out using solution blending[153–155]. In the *in-situ* polymerization method, inorganic fillers are suspended in the liquid phase of the monomer, and then the polymerization can occur around and between the filler particles. The reaction can be initiated either by incorporating an initiator curing agent or by thermal activation and UV irradiation (enzymatic initiation).

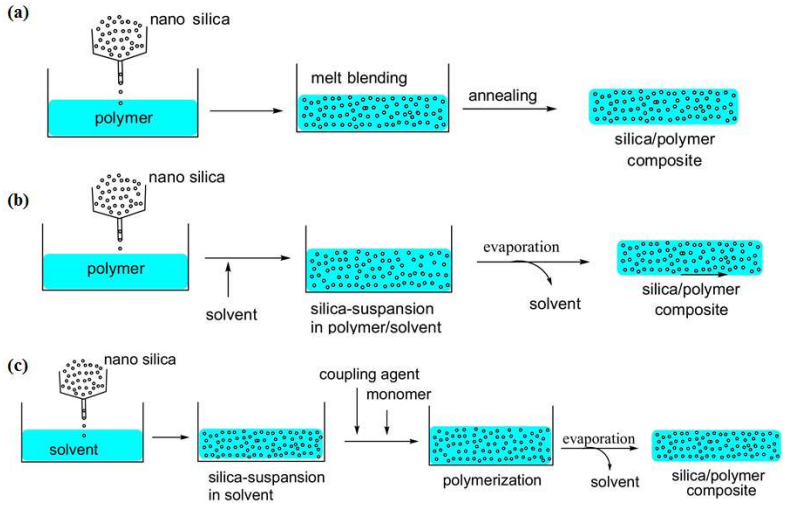

Figure 7. (a) Preparation processes of silica/polymer composites; **(a)** melt blending; **(b)** solution blending; and **(c)** *in-situ* polymerization method. Reproduced with permission from Elsevier[92].

Silica particles are used in functional coatings mainly in two forms: colloidal and fumed silica. Fumed silica, produced via flame hydrolysis, has been frequently used due to its significantly lower cost than colloidal silica. However, when dispersed, fumed silica tends to aggregate irreversibly. The preparation of colloidal silica particles usually follows the method introduced by Stöber, which consists of the hydrolysis and condensation of a silica precursor, such as tetraethyl orthosilicate (TEOS), in primary conditions[156]. Using this method, the particle size distribution is relatively narrow and tunable to different diameters, ranging from 20 nm to 1 μM. The films' silica content must be optimized to increase tensile strength and impact resistance simultaneously without decreasing flexural properties. A silica content of 10 wt% is usually found to give the best film properties[157,158].

3.1. Superhydrophobic coatings

Superhydrophobic surfaces have received considerable attention from fundamental research and practical applications[159]. Superhydrophobicity is defined as a water contact angle larger than 150° and contact angle hysteresis less than 10°, which is caused by the combined effect of both a hierarchical micro/nano-structure on the surface and a low surface energy[160–162]. Due to their water-repellent property, superhydrophobic surfaces have several emerging applications in a large number of fields, such as microfluidics[163], self-cleaning-fabrics[164], anti-icing materials[165,166], anti-fogging surfaces, anti-corrosive industrial parts and even surface drag reduction to reduce energy consumption in transport systems[167,168]. As an example, Bravo et al.[169] demonstrated a layer-by-layer processing scheme that can be utilized to create transparent superhydrophobic films from SiO_2 nanoparticles of various sizes. By controlling the placement and level of aggregation of differently sized SiO_2 nanoparticles within the resultant multilayer thin film, it is possible to optimize the level of surface roughness to achieve superhydrophobic behavior with limited light scattering. Transparent

superhydrophobic films were created by sequentially adsorbing silica nanoparticles and poly(allylamine hydrochloride). The final assembly was rendered superhydrophobic with a silane treatment, as shown in **Figure 8**.

Figure 8. Photograph of the glass slide coated with superhydrophobic multilayer based on silica nanoparticles and poly(allylamine hydrochloride). Reproduced with permission from the American Chemical Society[169].

Ming et al.[170] reported a robust procedure for preparing superhydrophobic films based on silica/polymer composites with an advancing contact angle for water of about 165° and the roll-off angle of a 10-μL water droplet is 3 ± 1°. Dual-size surface roughness mimics the surface topology of self-cleaning plant leaves originating from well-defined silica-based raspberry-like particles covalently bonded to an epoxy-based polymer matrix, as shown in **Figure 9**. The roughened surface is chemically modified with a layer of poly(dimethylsiloxane) (PDMS). The robustness and simplicity of this procedure would make widespread applications of so-prepared superhydrophobic films possible.

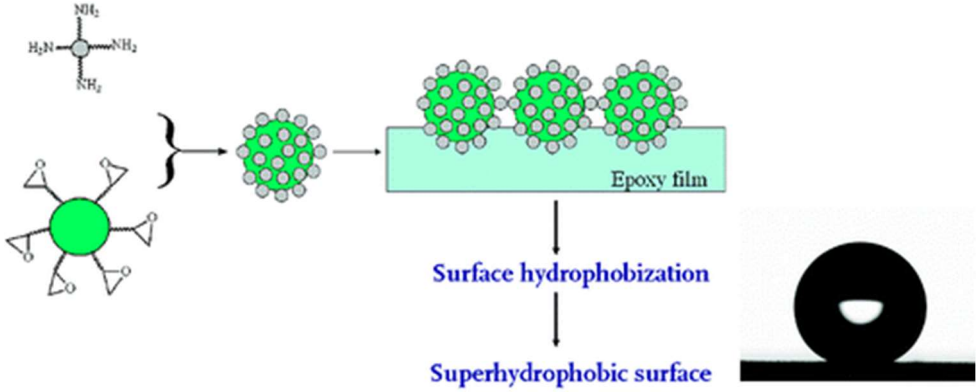

Figure 9. The schematic illustration is a superhydrophobic surface based on a silica/epoxy composite. Reproduced with permission from the American Chemical Society[170].

Superhydrophobic thermoplastic polyurethane (TPU) films based on octadecanamide (ODAA)-directed assembly of nanosilica/TPU/ODAA hybrids with a well-defined sheet-like microstructure were achieved by Yang et al.[171]. Such superhydrophobic surfaces showed improved mechanical robustness, and the procedures exhibited were facile and versatile. Tang et al.[172] reported superhydrophobic coatings based on two polymers, epoxy and acrylate copolymers, combined with silica nanoparticles.

3.2. Anti-reflective coatings

Anti-reflective films based on silica/polymer composites have been widely studied[173–177]. Lin et al.[178] reported anti-reflective silica/polymer composite coatings on glass and poly(methyl methacrylate) (PMMA) substrates. The coatings were prepared by silica mineralization of layer-by-layer (LbL) assembled films composed of polystyrene-block-poly(l-lysine)/poly(l-glutamic acid) (PS-b-PLL/PGA) complex vesicles

without any post-treatment. PS-b-PLL AB and A_2B block copolymers with appropriate block ratios can self-assemble to form vesicles, which can be deposited onto substrates without dissociation. Silica deposition, specifically onto the complex vesicles in the multilayer films through amine-catalyzed polycondensation, results in continuous, intact composite coatings comprising vesicular nanostructures, which provides an additional parameter for tuning their optical properties. The film thickness and porosity are mainly dictated by the bilayer number and the degree of deformation or fission of vesicles upon complexation and mineralization, depending on polymer composition. The coated PMMA substrate with maximum transmission over 98% can be achieved in the optimized wavelength region (**Figure 10**). The AR composite films were mechanically stable enough to withstand the wipe and adhesion tests due to the preparation of continuous, intact films.

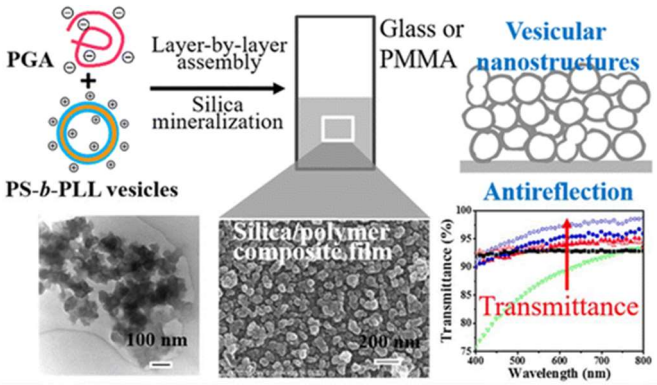

Figure 10. The anti-reflective coatings are based on silica/polymer composite film. Reproduced with permission from the American Chemical Society[178].

Xu et al.[179] reported anti-fogging and anti-reflection coatings based on silica nanoparticles and mesoporous silica nanoparticles onto glass and PMMA substrates via LbL assembly without post-treatments (**Figure 11**). A maximum transmittance of 98.5% in the visible spectral range was achieved for the coating deposited on slide glass. The maximum transmittance even reached as high as 99.3% by applying a coating to the PMMA substrate. The high porosity of mesoporous nanoparticles and loose stacking of solid and mesoporous nanoparticles are considered to contribute significantly to the enhancement of light.

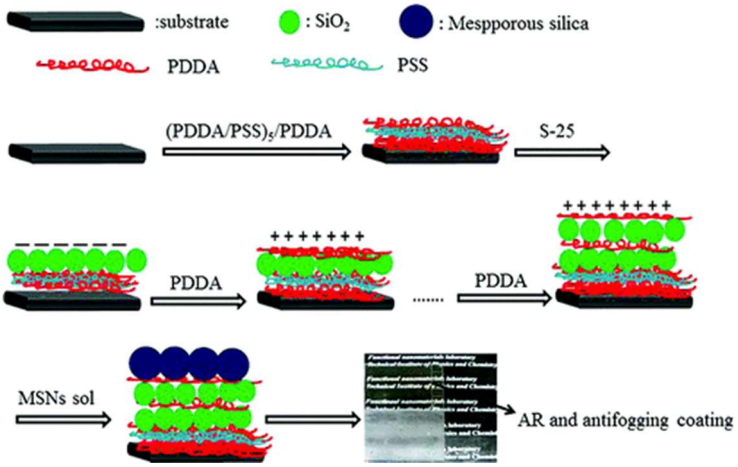

Figure 11. The anti-fogging and anti-reflective coatings were based on silica/polymer composite films fabricated by the LbL method. PSS-Sodium poly(4-styrene sulfonate); PDDA-poly(diallyldimethyl ammonium) chloride. Reproduced with permission from the American Chemical Society[179].

3.3. Anti-corrosive and protective coatings

Among a large number of reported organic-inorganic composite systems in which polymers such as epoxy, polyimide, acrylic, and polyethylenimine phases are combined with inorganic oxides such as silica, one important class is the PMMA-silica system. PMMA-silica nanocomposites have recently received considerable

attention because of their ability to protect a wide variety of metal surfaces, such as steels, stainless steels, aluminum alloys, and magnesium alloys, in an efficient and environmentally compliant manner[180–182]. These alloys are crucial for critical aerospace, automotive, and offshore industries. In the case of PMMA-silica hybrid nanocomposites, this corrosion protection is a consequence of the covalent bonding between PMMA and silica nodes through the coupling agent 3-(trimethoxysilyl)propyl methacrylate (MPTS), formed by three methoxy-silane groups linked by a nonhydrolysable Si-C bond to a methacrylate tail. This bonding mechanism produces a class II hybrid with a nanostructure of dense silica cross-link nodes bridged by short polymeric chains; consequently, the closely packed nanostructure acts as an efficient corrosion barrier against the uptake of aggressive agents.

4. Other applications

4.1. Proton exchange membranes

The proton exchange membrane (PEM) is one of the significant components in solid-type fuel cells, such as the proton exchange membrane fuel cell (PEMFC) and the direct methanol fuel cell (DMFC). Up to now, many research groups have reported the fabrication of polymer/silica nanocomposites as PEM[76,183–190]. Sulfonated poly(phthalazinone ether ketone) (sPPEK) with a degree of sulfonation of 1.23 was mixed with silica nanoparticles to form hybrid materials for use as PEMs[191,192]. The hybrid membranes exhibited improved swelling behavior, thermal stability, and mechanical properties. The methanol crossover behavior of the membrane was also depressed, such that these membranes were suitable for a high methanol concentration in the feed in a cell test. Sulfonated P(St-*co*-MA)-PEG/silica nanocomposite polyelectrolyte membranes were prepared with varied silica content using PEG of different molecular weights to have a fine control over spacing between silica domains, up to a few nanometers, by a chemically bound interior polymer chain[193]. Moreover, this system showed clear improvement over the Nafion membrane, as seen by selectivity parameter values due to low methanol permeability at 30 and 70 °C. In contrast, Nafion showed almost the same selectivity parameter values at both temperatures. The relatively high selectivity parameter values of these membranes at 70 °C indicated an excellent advantage for the composite over Nafion 117 membranes for targeting higher temperature applications.

Kanamura et al.[194] reported a new proton exchange membrane based on macroporous silica and a proton-conducting gel polymer electrolyte (**Figure 12**). 3D-uniformly ordered macroporous silica was synthesized using a colloidal template method with monodisperse polystyrene beads. A gel polymer, 2-acrylamido-2-methyl-1-propanesulfonic acid (AMPS), was injected into all the pores to prepare a proton-conducting membrane composite of macroporous silica and the gel polymer. The prepared membrane exhibited high proton conductivity and low methanol permeation. An H_2-O_2 fuel cell was constructed to test the composite membrane. The electrochemical performance obtained for the fuel cell with the composite membrane was similar to that for a fuel cell with a Nafion 117 membrane. From this result, it can be concluded that ceramic and polymer composite membranes can be applied to fuel cells working at low temperatures.

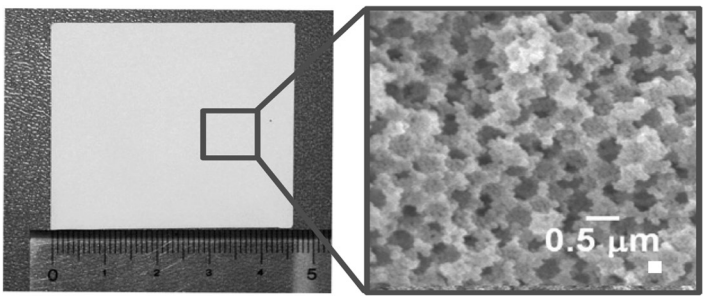

Figure 12. A new type of proton exchange membrane based on macroporous silica and a proton-conducting gel polymer electrolyte[194]. Reproduced with permission from the American Chemical Society.

4.2. Encapsulation for organic light-emitting devices

Direct encapsulation of organic light-emitting devices (OLEDs) is realized using highly transparent, photocurable *co*-polyacrylate/silica nanocomposite resin[195]. The feasibility of such a resin for OLED encapsulation was evaluated by physical/electrical property analysis of resins and driving voltage/luminance/lifetime measurement of OLEDs. Electrical property analysis revealed a higher electrical insulation of photocured nanocomposite resin film at 3.20×10^{12} Ω in comparison with that of oligomer film at 1.18×10^{12} Ω at 6.15 V to drive the bare OLED. This resulted in a lower leakage current, and the device driving voltage was efficiently reduced so that the nanocomposite-encapsulated OLED could be operated at a lower driving voltage of 6.09 V rather than 6.77 V for the oligomer-encapsulated OLED at the current density of 20 mA/cm^2. Luminance measurements revealed a luminance difference of less than 1.0% between OLEDs encapsulated by various types of resins, which indicated that the photopolymerization had a minimal effect on the light-emitting properties of OLEDs. Lifetime measurement of OLEDs found that t_{80}, the time span for the normalized luminance of the device, drops to 80% for nanocomposites-encapsulated OLED, which is 350.17 h in contrast to 16.83 h for bare OLED and 178.17 h for oligomer-encapsulated OLED. This demonstrated that nanocomposite resin with optimum properties was feasible for OLED packaging, and a compact device structure could be achieved via direct encapsulation.

4.3. CO_2 capture

Recently, silica/polymer composites have been exploited for CO_2-capturing applications[196–199]. Rezaei et al.[200] reported amine/silica/polymer composite hollow fiber adsorbents, which are produced using a novel reactive post-spinning infusion technique, and the fibers are shown to capture CO_2 from simulated flue gas (**Figure 13**). The post-spinning infusion technique allows for functionalizing polymer/ silica hollow fibers with different types of amines during the solvent exchange step after fiber spinning. The post-spinning infusion of 3-aminopropyltrimethoxysilane (APS) into mesoporous silica/cellulose acetate hollow fibers is demonstrated here, and the materials are compared with hollow fibers infused with poly(ethyleneimine) (PEI). This approach results in silica/polymer composite fibers with good amine distribution and accessibility and adequate porosity retained within the fibers to facilitate rapid mass transfer and adsorption kinetics. In contrast, fibers that are spun with presynthesized, amine-loaded mesoporous silica powders show negligible CO_2 uptake and low amine loadings because of the loss of amines from the silica materials during the fiber spinning process. Aminosilica powders are shown to be more hydrophilic than the corresponding amine-containing composite hollow fibers, the bare polymer, as silica supports. The PEI-infused and APS-infused fibers demonstrate reduced CO_2 adsorption upon elevating the temperature from 35 to 80 °C, per thermodynamics. In contrast, PEI-infused powders show increased CO_2 uptake over that temperature range because of competing diffusional and thermodynamic effects. The results indicate the post-spinning infusion method provides a new platform for synthesizing composite polymer/silica/amine fibers that may facilitate the ultimate scale-up of practical fiber adsorbents for flue gas CO_2 capture applications.

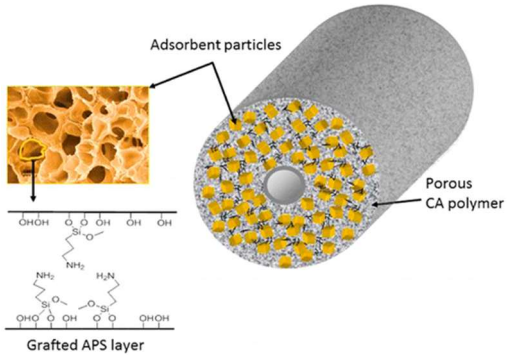

Figure 13. Amine/silica/polymer composite hollow fiber adsorbents[200]. Reproduced with permission from the American Chemical Society.

4.4. Sensors

Silica/polymer composites have been widely studied for various sensing applications[201–205]. An approach for preparing polydiacetylene/silica nanocomposites for use as a chemosensor was reported[62]. The disordered 10,12-pentacosadiynoic acid (PCDA) aggregates could be absorbed on the surfaces of silica nanoparticles in an aqueous solution. The disordered PCDA molecules in aggregates were turned into an ordered arrangement with the help of a silica nanoparticle template. After irradiation with UV light, polydiacetylene/silica nanocomposites took on a blue color. Various environmental perturbations, such as temperature, pH, and amphiphilic molecules, could result in a colorimetric change of the polydiacetylene/silica nanocomposites from the blue to the red phase. The material may find some interesting potential applications as a new chemosensor.

4.5. Metal uptake

The nanocomposites of electroactive polymers PANI or PPy with ultrafine SiO_2 particles have potential commercial applications for metal uptake based on the fact that they possess a surface area substantially higher than that estimated from the particle size and hence can aid the process of metal uptake. The use of electroactive polymer/SiO_2 nanocomposites to uptake gold and palladium from $AuCl_3$ and $PdCl_2$ in acid solutions, respectively, was investigated[53]. In the case of gold uptake, the reaction rate increased with temperature from 0 to 60 °C. The accumulation of elemental gold on the nanocomposites increased the diameter and decreased the surface area. The surface Au/N ratio, as determined using XPS, was highly dependent on the rate of reactions, even for the same amount of gold uptake. The uptake of palladium from $PdCl_2$ was much more challenging to accomplish. High uptake rates could only be achieved with the electroactive polymers reduced to their lowest oxidation state. Unlike the case of gold uptake, the palladium on the microparticles did not exist in the elemental form but as a Pd(II) compound.

5. Functional materials based on sand

5.1. Proppants

A proppant can be defined as a solid material, usually sand or modified sand, designed to keep the induced hydraulic fracture open to extract gaseous products from the fracture. The so-called frac sand is easily friable and creates fines when over-stressed; modified sand with polymers or resins was developed to enhance the conductivity of frac sand. The main advantage of using resin to coat the proppant is that the resin coating can trap pieces of broken grain within the coating, thereby preventing proppant flow back to the wellbore (**Figure 14**). They could also connect individual proppant grains to avoid the proppant flowing back. In this way, they are commonly used in the tail-in-fracturing process. The details of different types of proppants and their functions, developed and used in the oil and gas industries, can be found elsewhere[206,207]. The resin-coated proppants can also prevent sand production in areas of soft formation where sand control is needed[208–211]. The resin coat can be pre-cured or curable. In general, uncured resin systems have poor mechanical properties. However, good properties are obtained by reacting the linear resin with suitable curatives to form 3D-cross-linked thermoset structures. This process is commonly referred to as curing. Pre-cured, resin-coated sand is processed by applying the resin to the sand. No further curing will take place downhole. For curable resin-coated proppant, the well is shut in after fracturing to allow curing—the curing process results in a consolidated proppant bed with a cured resin coating surrounding each proppant grain. The performance of the proppant depends on the properties of the cured resin material. The chemical cross-links that form during the resin cure do not allow the cured material to melt or flow when re-heated. However, cured/cross-linked resins undergo a very slight softening at elevated temperatures at a point of T_g. When the temperature is above the T_g, the mobility of the polymer chains increases significantly, and the cured resin changes from a rigid/glassy state to

a rubbery/compliant state. In this case, the resin system becomes soft, decreasing strength. Therefore, the T_g has been used as a valuable parameter to determine the upper-performance limit of the resin.

The most commonly used resins used to coat proppants are epoxy resins, furan, polyesters, vinyl esters, and polyurethane[207]. Epoxy resin is the primary polymer type used for proppant coating because it has excellent mechanical strength, heat resistance, and chemical resistance.

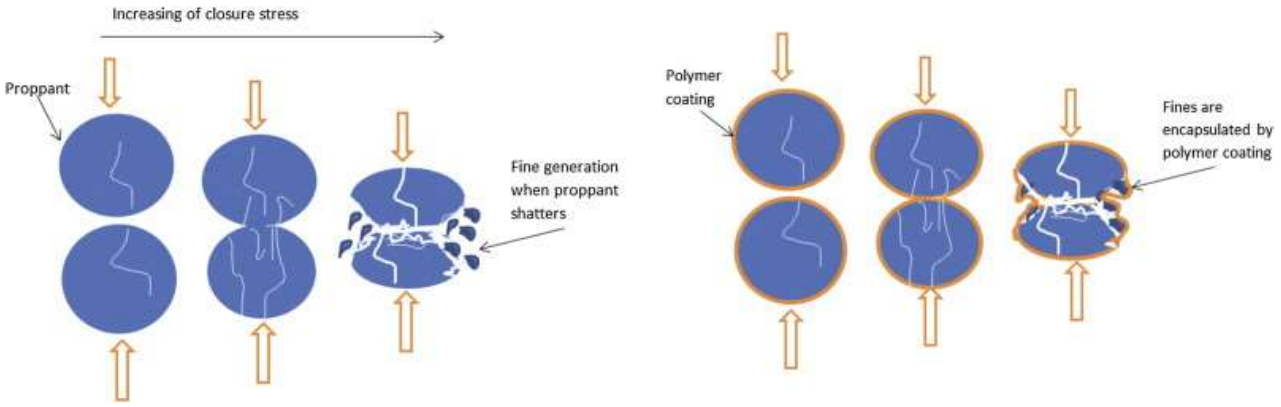

Figure 14. The schematic illustration of fine production in unmodified and modified (polymer coated) proppants under closure stress[207,212]. Reproduced with permission from Elsevier.

5.2. Superhydrophobic sand

"Superhydrophobic sand" has recently been studied for various potential applications[213–215]. Superhydrophobic sand has been proposed to realize the storage and transportation of the surface water of sandy soils, especially in deserts[214,216]. Sand dunes are an abundant natural resource in the desert, are characterized by a low water storage capacity, and suffer from a temporary water shortage, mainly when cultivated under arid conditions. Sand consists of hydrophilic silica, which attracts water and facilitates its flow to the ground, thus adversely affecting the plantation, even under expensive irrigation systems such as sprinkling or trickling. Previously, hydrogels were used to increase the water-holding capacity of sandy soils[217–219]. Recently, it has been proposed that applying nanomaterials to the sand surface can combat desertification and encourage plant growth in arid climates. Moreover, superhydrophobic sand prevents the diffusion of underground salt, affecting plants' growth. Applying the superhydrophobic properties of certain nanomaterials to mitigating environmental and resource issues is a promising research topic of global significance. The development of low-cost, environmentally friendly, superhydrophobic, thermally stable, and promising adhesion nanomaterials is a challenge for desert greening.

Chen et al.[220] reported the preparation of three kinds of hydrophobic sands with different surface structures and wettability by cladding inorganic materials of nonmetal (SiO_2) and metal (Ag and Cu) on sand surfaces and then modifying them with low-surface-energy chemicals (**Figure 15**). Combining the superhydrophobicity with the desert sand, superhydrophobic sand (PFDS-sand@SiO_2) is shown to have excellent water repellency, meaning that the water can stably stay and flow on such a sand surface without any wetting or permeation, and has such excellent water-holding capacity that a sand layer with a 2 cm thickness can sustain a water column height of 35 cm. Significantly, such superhydrophobic sand, PFDS-sand@SiO_2, exhibits exceptionally high thermal stability up to 400 ºC when used for water storage. This result is unprecedented and enough to face the high-temperature conditions of the desert and some others.

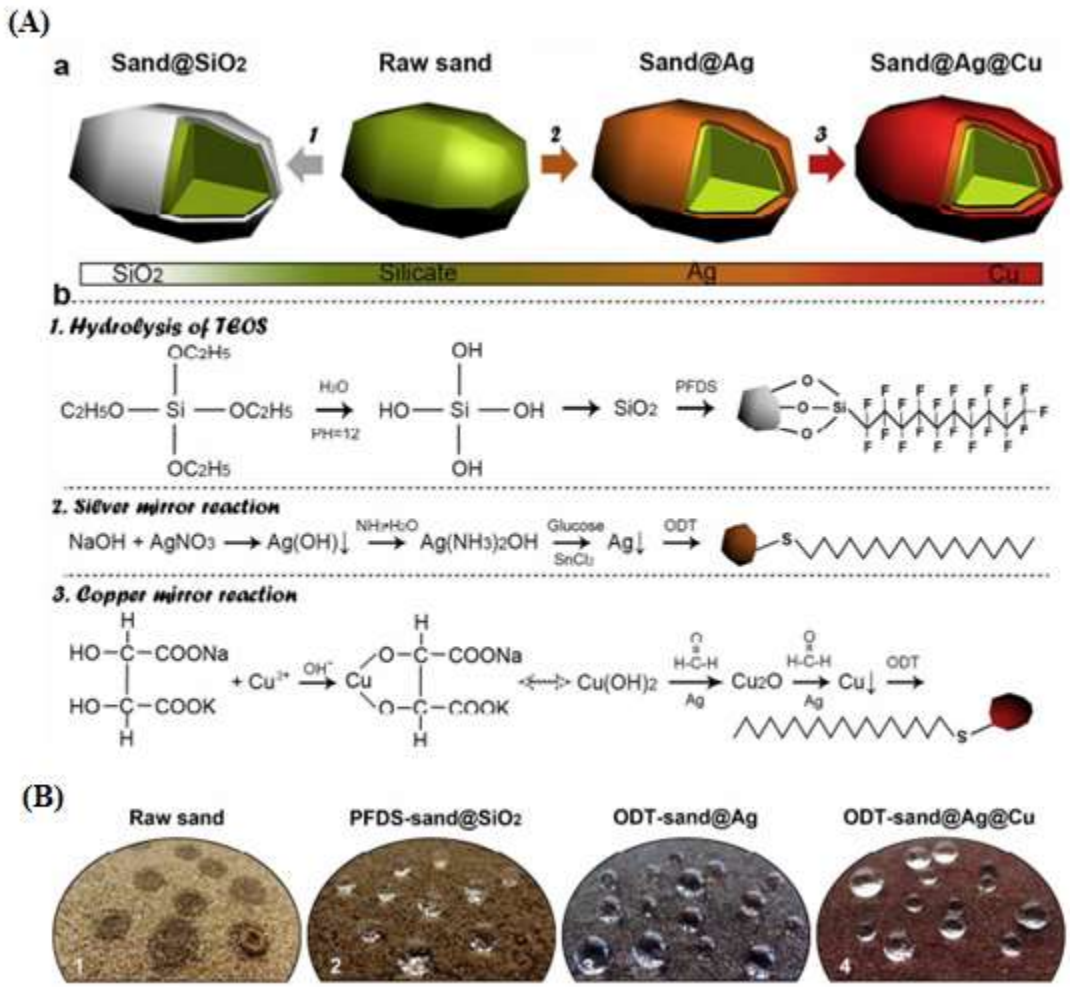

Figure 15. (A) The preparation of superhydrophobic sands. **(a)** Schematic illustration of the surface modifications of the sand; **(b)** the chemical reactions of the surface modifications of the sand. **(B)** The wettability and water repellency of the prepared superhydrophobic sands[220]. Reproduced with permission from the Royal Society of Chemistry.

5.3. Nanosand-based functional materials

Nanosand derived from highly abundant and low-cost sand through nanomilling has attracted the great interest of researchers recently, as it finds various potential applications, including as a critical component in nanofluids[221,222], water filtration membranes[223], as a nanofiller[224–229], and polypropylene-based composites[230]. In addition, nanostructured sand is found to be a potential candidate for oil recovery in produced water treatment and pollutant absorption[231]. Manikandan et al.[222] reported the stable dispersions of nanosand with propylene glycol (P.G.), an excellent coolant system for heat transfer management in various manufacturing units. Similarly, they have also studied the sub-micron-sized sand dispersion in water as a nanofluid[221]. The stable dispersion of nanoparticles in a liquid, stabilized either by electrostatic or steric interaction, has provided a practical method of improving the thermal conductivity of conventional coolant through particle addition. Such stable dispersions are referred to as nanofluids. Nanosand-water or nanosand-propylene glycol dispersions have a higher thermal conductivity ratio than silica-water nanofluids reported in the literature. Stable nanosand-PG nanofluids were formulated by dispersing nanosands of 20–25 nm particle size produced by stirred bead milling in P.G. through extended probe ultrasonication. The viscosity of nanosand-PG nanofluids decreases with the concentration of nanosand and temperature. In the well-dispersed nanosand-PG, the interactions between nanoparticles and P.G. through the nanoparticle surface led to disturbance of the hydrogen bonding network of P.G. This results in a reduction in the viscosity of the nanofluid in comparison to pure P.G. For instance, the viscosity of 2 vol% nanosand-PG nanofluid is found to be 46% lower than that of pure P.G. at 29 °C.

Nanosand has been introduced into epoxy resin for its good toughness and mechanical strength. The nanosand exhibited good compatibility with the epoxy matrix, and the dispersion and concentration of the nanosand determined the enhancement. Both flexural strength and fracture toughness have been greatly improved by incorporating 3 wt% nanosand. The addition of nanosand to epoxy changes the curing reaction and the T_g. The nanosand has been used without any further surface treatment, resulting in a lot of hydroxyl groups (-OH) groups and, hence, better chemical interaction with the epoxy resin and better properties of the composites.

6. Summary and outlook

Recently, more research has been published on silica or sand/polymer composites aimed at various potential applications. The composites' current status and recent application developments have been summarized. The different preparation methods of silica and polymer have been extensively investigated. However, the properties of polymer/silica nanocomposites are generally superior to those of pure polymer matrixes and polymer microcomposites. Multi-functional coatings based on silica/polymer composite materials combine the flexural properties and processability of the polymer with a varied array of properties that the inorganic components can impart. Silica nanoparticles are among the most commonly used for composite coating applications. These not only provide increased tensile strength, scratch resistance, and impact resistance but are also extremely versatile vehicles to incorporate other components, which, in turn, open the possibility of obtaining coatings with a wide range of new properties. Most of the properties and potential functionalities of these silica/polymer composites are dependent on a homogeneous distribution of the organic and inorganic components. For example, functionalized polymer nanoparticles can serve as a template to prepare silica composite films with a hierarchical structure to obtain superhydrophobic and amphiphobic coatings for self-cleaning surfaces. The silica nanoparticles are incorporated in a polymer matrix in most of the of the described applications. Due to mixability issues of the silica with most polymers, this requires the surface functionalization of the silica to achieve good compatibility between the two components and, thus, avoid the aggregation of the silica particles in the final material. Using composite nanoparticles with a silica core and a polymer shell can obtain perfectly homogeneous particle distributions and further control the spacing between silica particles in the final material, which might be necessary for many applications[16,43,232–239]. The facile oil-water separation, absorption, and CO_2 capture by the silica/polymer composites are promising in overcoming recent environmental issues. Very interestingly, considerable efforts have been made to realize agriculture in deserts through superhydrophobic sand (**Figure 16**). All these manifestations imply the significant potential of such superhydrophobic sand in its application to desert water storage and transportation. The facile and economical preparation methods of the superhydrophobic sand would be a big hope in achieving the most challenging water storage and transport in Middle Eastern countries.

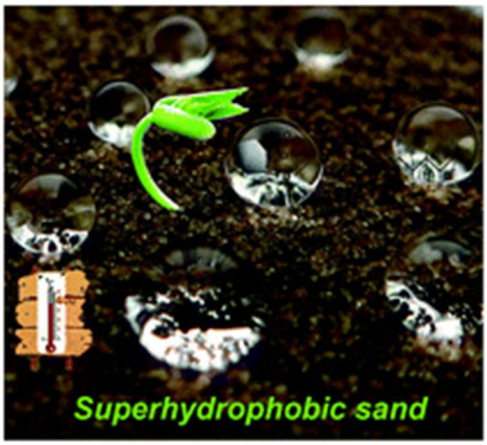

Figure 16. A photograph depicts the realization of agriculture through superhydrophobic sand in deserts[220]. Reproduced with permission from the Royal Society of Chemistry.

Acknowledgments

This study is part of research project agreement no. AFU-01-2017 in collaboration with EXPEC Advanced Research Centre, Saudi Aramco. The authors gratefully acknowledge the continued support from AlFaisal University and its Office of Research.

Conflict of interest

All authors declare no conflict of interest.

References

1. Shannon MA, Bohn PW, Elimelech M, et al. Science and technology for water purification in the coming decades. *Nature* 2008; 452: 301–310. doi: 10.1038/nature06599
2. Guerin TF. Heavy equipment maintenance wastes and environmental management in the mining industry. *Journal of Environmental Management* 2002; 66(2): 185–199. doi: 10.1006/jema.2002.0583
3. Gupta RK, Dunderdale GJ, England MW, Hozumi A. Oil/water separation techniques: A review of recent progresses and future directions. *Journal of Materials Chemistry A* 2017; 5(31): 16025–16058. doi: 10.1039/C7TA02070H
4. Gaaseidnes K, Turbeville J. Separation of oil and water in oil spill recovery operations. *Pure and Applied Chemistry* 1999; 71(1): 95–101. doi: 10.1351/pac199971010095
5. Wayment EC, Wagstaff B. Appropriate technology for oil spill management in developing nations. *Pure and Applied Chemistry* 1999; 71(1): 203–208. doi: 10.1351/pac199971010203
6. Lai J-C, Jia X-Y, Wang D-P, et al. Thermodynamically stable whilst kinetically labile coordination bonds lead to strong and tough self-healing polymers. *Nature Communications* 2019; 10: 1164. doi: 10.1038/s41467-019-09130-z
7. Hu Y, Liu X, Zou J, et al. Graphite/isobutylene-isoprene rubber highly porous cryogels as new sorbents for oil spills and organic liquids. *ACS Applied Materials & Interfaces* 2013; 5(16): 7737–7742. doi: 10.1021/am303294m
8. Wu J, Wang N, Wang L, et al. Electrospun porous structure fibrous film with high oil adsorption capacity. *ACS Applied Materials & Interfaces* 2012; 4(6): 3207–3212. doi: 10.1021/am300544d
9. Zhu Q, Chu Y, Wang Z, et al. Robust superhydrophobic polyurethane sponge as a highly reusable oil-absorption material. *Journal of Materials Chemistry A* 2013; 1(17): 5386–5393. doi: 10.1039/C3TA00125C
10. Prathap A, Sureshan KM. A mannitol based phase selective supergelator offers a simple, viable and greener method to combat marine oil spills. *Chemical Communications* 2012; 48(43): 5250–5252. doi: 10.1039/C2CC31631E
11. Li C-H, Wang C, Keplinger C, et al. A highly stretchable autonomous self-healing elastomer. *Nature Chemistry* 2016; 8: 618–624. doi: 10.1038/nchem.2492
12. Zhu D, Handschuh-Wang S, Zhou X. Recent progress in fabrication and application of polydimethylsiloxane sponges. *Journal of Materials Chemistry A* 2017; 5(32): 16467–16497. doi: 10.1039/C7TA04577H
13. Zhang A, Chen M, Du C, et al. Poly(dimethylsiloxane) oil absorbent with a three-dimensionally interconnected porous structure and swellable skeleton. *ACS Applied Materials & Interfaces* 2013; 5(20): 10201–10206. doi: 10.1021/am4029203
14. Krishnan MR, Aldawsari YF, Alsharaeh EH. Three-dimensionally cross-linked styrene-methyl methacrylate-divinyl benzene terpolymer networks for organic solvents and crude oil absorption. *Journal of Applied Polymer Science* 2021; 138(9): 49942. doi: 10.1002/app.49942
15. Krishnan MR, Aldawsari YF, Alsharaeh EH. 3D-poly(styrene-methyl methacrylate)/divinyl benzene-2D-nanosheet composite networks for organic solvents and crude oil spill cleanup. *Polymer Bulletin* 2021; 79: 3779–3802. doi: 10.1007/s00289-021-03565-5
16. Krishnan MR, Almohsin A, Alsharaeh EH. Syntheses and fabrication of mesoporous styrene-co-methyl methacrylate-graphene composites for oil removal. *Diamond and Related Materials* 2022; 130: 109494. doi: 10.1016/j.diamond.2022.109494
17. Krishnan MR, Samitsu S, Fujii Y, Ichinose I. Hydrophilic polymer nanofibre networks for rapid removal of aromatic compounds from water. *Chemical Communications* 2014; 50(66): 9393–9396. doi: 10.1039/C4CC01786B
18. Samitsu S, Zhang R, Peng X, et al. Flash freezing route to mesoporous polymer nanofibre networks. *Nature Communications* 2013; 4: 2653. doi: 10.1038/ncomms3653
19. Syazmin NA, Shahadat M, Razali MR, Adnan R. PDMS-supported composite materials as oil absorbent. In: Shahid-ul-Islam, Shalla AH, Shahadat M (editors). *Green Chemistry for Sustainable Water Purification*. Scrivener Publishing LLC; 2023. p. 203–221. doi: 10.1002/9781119852322.ch9
20. Uragami T. Structural design of polymer membranes for concentration of bio-ethanol. *Polymer Journal* 2008; 40: 485–494. doi: 10.1295/polymj.PJ2008015

21. Whitesides GM. The origins and the future of microfluidics. *Nature* 2006; 442: 368–373. doi: 10.1038/nature05058
22. Xia Y, Whitesides GM. Soft lithography. *Angewandte Chemie International Edition* 1998; 37(5): 550–575. doi: 10.1002/%28SICI%291521-3773%2819980316%2937%3A5<550%3A%3AAID-ANIE550>3.0.CO%3B2-G
23. Bélanger M, Marois Y. Hemocompatibility, biocompatibility, inflammatory and in vivo studies of primary reference materials low-density polyethylene and polydimethylsiloxane: A review. *Journal of Biomedical Materials Research* 2001; 58(5): 467–477. doi: 10.1002/jbm.1043
24. Mata A, Fleischman AJ, Roy S. Characterization of polydimethylsiloxane (PDMS) properties for biomedical micro/nanosystems. *Biomedical Microdevices* 2005; 7: 281–293. doi: 10.1007/s10544-005-6070-2
25. Yilgör E, Yilgör I. Silicone containing copolymers: Synthesis, properties and applications. *Progress in Polymer Science* 2014; 39(6): 1165–1195. doi: 10.1016/j.progpolymsci.2013.11.003
26. Dong C-H, He L, Xiao Y-F, et al. Fabrication of high-Q polydimethylsiloxane optical microspheres for thermal sensing. *Applied Physics Letters* 2009; 94(23): 231119. doi: 10.1063/1.3152791
27. Quake SR, Scherer A. From micro- to nanofabrication with soft materials. *Science* 2000; 290(5496): 1536–1540. doi: 10.1126/science.290.5496.1536
28. Lee JN, Park C, Whitesides GM. Solvent compatibility of poly(dimethylsiloxane)-based microfluidic devices. *Analytical Chemistry* 2003; 75(23): 6544–6554. doi: 10.1021/ac0346712
29. Zhou X, Lau L, Lam WWL, et al. Nanoliter dispensing method by degassed poly(dimethylsiloxane) microchannels and its application in protein crystallization. *Analytical Chemistry* 2007; 79(13): 4924–4930. doi: 10.1021/ac070306p
30. Zhou X, Li J, Wu C, Zheng B. Constructing the phase diagram of an aqueous solution of poly(N-isopropyl acrylamide) by controlled microevaporation in a nanoliter microchamber. *Macromolecular Rapid Communications* 2008; 29(16): 1363–1367. doi: 10.1002/marc.200800229
31. Chen I-J, Lindner E. The stability of radio-frequency plasma-treated polydimethylsiloxane surfaces. *Langmuir* 2007; 23(6): 3118–3122. doi: 10.1021/la0627720
32. Hu S, Ren X, Bachman M, et al. Tailoring the surface properties of poly(dimethylsiloxane) microfluidic devices. *Langmuir* 2004; 20(13): 5569–5574. doi: 10.1021/la049974l
33. Zhou J, Ellis AV, Voelcker NH. Recent developments in PDMS surface modification for microfluidic devices. *ELECTROPHORESIS* 2010; 31(1): 2–16. doi: 10.1002/elps.200900475
34. Bauer WAC, Fischlechner M, Abell C, Huck WTS. Hydrophilic PDMS microchannels for high-throughput formation of oil-in-water microdroplets and water-in-oil-in-water double emulsions. *Lab on a Chip* 2010; 10(14): 1814–1819. doi: 10.1039/C004046K
35. Li X, Tanyan S, Xie S, et al. A 3D porous PDMS sponge embedded with carbon nanoparticles for solar driven interfacial evaporation. *Separation and Purification Technology* 2022; 292: 120985. doi: 10.1016/j.seppur.2022.120985
36. Yang X-Y, Chen L-H, Li Y, et al. Hierarchically porous materials: Synthesis strategies and structure design. *Chemical Society Reviews* 2017; 46(2): 481–558. doi: 10.1039/C6CS00829A
37. Das S, Heasman P, Ben T, Qiu S. Porous organic materials: Strategic design and structure–function correlation. *Chemical Reviews* 2017; 117(3): 1515–1563. doi: 10.1021/acs.chemrev.6b00439
38. Wu D, Xu F, Sun B, et al. Design and preparation of porous polymers. *Chemical Reviews* 2012; 112(7): 3959–4015. doi: 10.1021/cr200440z
39. Jiang W, Zhu Y, Zhu G, et al. Three-dimensional photocatalysts with a network structure. *Journal of Materials Chemistry A* 2017; 5(12): 5661–5679. doi: 10.1039/C7TA00398F
40. Yu M, Qiu W, Wang F, et al. Three dimensional architectures: Design, assembly and application in electrochemical capacitors. *Journal of Materials Chemistry A* 2015; 3(31): 15792–15823. doi: 10.1039/C5TA02743H
41. Krishnan MR, Almohsin A, Alsharaeh EH. Mechanically robust and thermally enhanced sand-polyacrylamide-2D nanofiller composite hydrogels for water shutoff applications. *Journal of Applied Polymer Science* 2023. doi: 10.1002/app.54953
42. Krishnan MR, Li W, Alsharaeh EH. Cross-linked polymer nanocomposite networks coated nano sand light-weight proppants for hydraulic fracturing applications. *Characterization and Application of Nanomaterials* 2023; 6(2): 3314. doi: 10.24294/can.v6i2.3314
43. Krishnan MR, Alsharaeh EH. Polymer gel amended sandy soil with enhanced water storage and extended release capabilities for sustainable desert agriculture. *Journal of Polymer Science and Engineering* 2023; 6(1): 2892. doi: 10.24294/jpse.v6i1.2892
44. Sanchez C, Belleville P, Popall M, Nicole L. Applications of advanced hybrid organic–inorganic nanomaterials: from laboratory to market. *Chemical Society Reviews* 2011; 40(2): 696–753. doi: 10.1039/C0CS00136H
45. Zou H, Wu S, Shen J. Polymer/silica nanocomposites: Preparation, characterization, properties, and applications. *Chemical Reviews* 2008; 108(9): 3893–3957. doi: 10.1021/cr068035q
46. Wei L, Hu N, Zhang Y. Synthesis of polymer—Mesoporous silica nanocomposites. *Materials* 2010; 3(7): 4066–4079. doi: 10.3390/ma3074066

47. Kickelbick G. Concepts for the incorporation of inorganic building blocks into organic polymers on a nanoscale. *Progress in Polymer Science* 2003; 28(1): 83–114. doi: 10.1016/S0079-6700(02)00019-9
48. Paul DR, Robeson LM. Polymer nanotechnology: Nanocomposites. *Polymer* 2008; 49(15): 3187–3204. doi: 10.1016/j.polymer.2008.04.017
49. Yang F, Nelson GL. Polymer/silica nanocomposites prepared via extrusion. *Polymers for Advanced Technologies* 2006; 17(4): 320–326. doi: 10.1002/pat.695
50. Ke Y, Stroeve P. *Polymer-layered Silicate and Silica Nanocomposites*. Elsevier Science; 2005. doi: 10.1016/B978-0-444-51570-4.X5000-9
51. Peters ST (editor). *Handbook of Composites*. Springer New York; 2013. doi: 10.1007/978-1-4615-6389-1
52. Yin P, Xu M, Liu W, et al. High efficient adsorption of gold ions onto the novel functional composite silica microspheres encapsulated by organophosphonated polystyrene. *Journal of Industrial and Engineering Chemistry* 2014; 20(2): 379–390. doi: 10.1016/j.jiec.2013.04.032
53. Neoh KG, Tan KK, Goh PL, et al. Electroactive polymer–SiO_2 nanocomposites for metal uptake. *Polymer* 1999; 40(4): 887–893. doi: 10.1016/S0032-3861(98)00297-3
54. Javadian H, Sorkhrodi FZ, Koutenaei BB. Experimental investigation on enhancing aqueous cadmium removal via nanostructure composite of modified hexagonal type mesoporous silica with polyaniline/polypyrrole nanoparticles. *Journal of Industrial and Engineering Chemistry* 2014; 20(5): 3678–3688. doi: 10.1016/j.jiec.2013.12.066
55. Setshedi KZ, Bhaumik M, Onyango MS, Maity A. Breakthrough studies for Cr(VI) sorption from aqueous solution using exfoliated polypyrrole-organically modified montmorillonite clay nanocomposite. *Journal of Industrial and Engineering Chemistry* 2014; 20(4): 2208–2216. doi: 10.1016/j.jiec.2013.09.052
56. Taha AA, Wu Y, Wang H, Li F. Preparation and application of functionalized cellulose acetate/silica composite nanofibrous membrane via electrospinning for Cr(VI) ion removal from aqueous solution. *Journal of Environmental Management* 2012; 112: 10–16. doi: 10.1016/j.jenvman.2012.05.031
57. Mirzabe GH, Keshtkar AR. Application of response surface methodology for thorium adsorption on PVA/Fe_3O_4/SiO_2/APTES nanohybrid adsorbent. *Journal of Industrial and Engineering Chemistry* 2015; 26: 277–285. doi: 10.1016/j.jiec.2014.11.040
58. Rosenberg E. Silica polyamine composites: Advanced materials for metal ion recovery and remediation. In: Abd-El-Aziz AS, Carraher Jr. CE, Pittman Jr. CU, Zeldin M (editors). *Macromolecules Containing Metal and Metal-Like Elements*. John Wiley & Sons, Inc.; 2005. p. 51–78. doi: 10.1002/0471712566.ch4
59. Samart C, Prawingwong P, Amnuaypanich S, et al. Preparation of poly acrylic acid grafted-mesoporous silica as pH responsive releasing material. *Journal of Industrial and Engineering Chemistry* 2014; 20(4): 2153–2158. doi: 10.1016/j.jiec.2013.09.045
60. Pourjavadi A, Tehrani ZM, Jokar S. Functionalized mesoporous silica-coated magnetic graphene oxide by polyglycerol-g-polycaprolactone with pH-responsive behavior: Designed for targeted and controlled doxorubicin delivery. *Journal of Industrial and Engineering Chemistry* 2015; 28: 45–53. doi: 10.1016/j.jiec.2015.01.021
61. Jang J, Ha J, Lim B. Synthesis and characterization of monodisperse silica–polyaniline core–shell nanoparticles. Chemical Communications 2006; 2006(15): 1622–1624. doi: 10.1039/B600167J
62. Su Y-L. Preparation of polydiacetylene/silica nanocomposite for use as a chemosensor. *Reactive and Functional Polymers* 2006; 66(9): 967–973. doi: 10.1016/j.reactfunctpolym.2006.01.021
63. Wong CP, Bollampally RS. Thermal conductivity, elastic modulus, and coefficient of thermal expansion of polymer composites filled with ceramic particles for electronic packaging. *Journal of Applied Polymer Science* 1999; 74(14): 3396–3403. doi: 10.1002/(SICI)1097-4628(19991227)74:14<3396::AID-APP13>3.0.CO;2-3
64. Gonon P, Sylvestre A, Teysseyre J, Prior C. Dielectric properties of epoxy/silica composites used for microlectronic packaging, and their dependence on post-curing. *Journal of Materials Science: Materials in Electronics* 2001; 12: 81–86. doi: 10.1023/A:1011241818209
65. Devoldere N, Bosc D, Loisel B. Mixed Silica/Polymer Active Directional Coupler, in Integrated Optics. U.S. Patent US5,857,039A, 5 January 1999.
66. Jiguet S, Bertsch A, Hofmann H, Renaud P. Conductive SU8 photoresist for microfabrication. *Advanced Functional Materials* 2005; 15(9): 1511–1516. doi: 10.1002/adfm.200400575
67. Jang J-H, Ullal CK, Maldovan M, et al. 3D micro- and nanostructures via interference lithography. *Advanced Functional Materials* 2007; 17(16): 3027–3041. doi: 10.1002/adfm.200700140
68. Cho J-D, Ju H-T, Park Y-S, Hong J-W. Kinetics of cationic photopolymerizations of UV-curable epoxy-based SU8-negative photoresists with and without silica nanoparticles. *Macromolecular Materials and Engineering* 2006; 291(9): 1155–1163. doi: 10.1002/mame.200600124
69. Battaglin G, Cattaruzza E, Gonella F, et al. Structural and optical properties of Cu:silica nanocomposite films prepared by co-sputtering deposition. *Applied Surface Science* 2004; 226(1–3): 52–56. doi: 10.1016/j.apsusc.2003.11.030
70. Yu Y-Y, Chen W-C. Transparent organic–inorganic hybrid thin films prepared from acrylic polymer and aqueous monodispersed colloidal silica. *Materials Chemistry and Physics* 2003; 82(2): 388–395. doi: 10.1016/S0254-0584(03)00259-1
71. Chang C-C, Chen W-C. Synthesis and optical properties of polyimide-silica hybrid thin films. *Chemistry of Materials* 2002; 14(10): 4242–4248. doi: 10.1021/cm0202310

72. Kashiwagi T, Morgan AB, Antonucci JM, et al. Thermal and flammability properties of a silica–poly(methylmethacrylate) nanocomposite. *Journal of Applied Polymer Science* 2003; 89(8): 2072–2078. doi: 10.1002/app.12307
73. Chiang C-L, Ma C-CM. Synthesis, characterization, and properties of novel ladderlike phosphorus-containing polysilsesquioxanes. *Journal of Polymer Science, Part A: Polymer Chemistry* 2003; 41(9): 1371–1379. doi: 10.1002/pola.10684
74. Mishra AK, Kuila T, Kim D-Y, et al. Protic ionic liquid-functionalized mesoporous silica-based hybrid membranes for proton exchange membrane fuel cells. *Journal of Materials Chemistry* 2012; 22(46): 24366–24372. doi: 10.1039/C2JM33288D
75. Jang S-Y, Han S-H. Sulfonated polySEPS/hydrophilic-SiO_2 composite membranes for polymer electrolyte membranes (PEMs). *Journal of Industrial and Engineering Chemistry* 2015; 23: 285–289. doi: 10.1016/j.jiec.2014.08.030
76. Wang H, Holmberg BA, Huang L, et al. Nafion-bifunctional silica composite proton conductive membranes. *Journal of Materials Chemistry* 2002; 12(4): 834–837. doi: 10.1039/B107498A
77. Liu H, Gong C, Wang J, et al. Chitosan/silica coated carbon nanotubes composite proton exchange membranes for fuel cell applications. *Carbohydrate Polymers* 2016; 136: 1379–1385. doi: 10.1016/j.carbpol.2015.09.085
78. Kim DJ, Jo MJ, Nam SY. A review of polymer–nanocomposite electrolyte membranes for fuel cell application. *Journal of Industrial and Engineering Chemistry* 2015; 21: 36–52. doi: 10.1016/j.jiec.2014.04.030
79. Weng C-J, Chang C-H, Lin I-L, et al. Advanced anticorrosion coating materials prepared from fluoro-polyaniline-silica composites with synergistic effect of superhydrophobicity and redox catalytic capability. *Surface and Coatings Technology* 2012; 207: 42–49. doi: 10.1016/j.surfcoat.2012.04.097
80. Ghanbari A, Attar MM. A study on the anticorrosion performance of epoxy nanocomposite coatings containing epoxy-silane treated nano-silica on mild steel substrate. *Journal of Industrial and Engineering Chemistry* 2015; 23: 145–153. doi: 10.1016/j.jiec.2014.08.008
81. Golestaneh M, Amini G, Najafpour GD, Beygi MA. Evaluation of mechanical strength of epoxy polymer concrete with silica powder as filler. *World Applied Sciences Journal* 2010; 9(2): 216–220.
82. Yeh J-M, Chang K-C. Polymer/layered silicate nanocomposite anticorrosive coatings. *Journal of Industrial and Engineering Chemistry* 2008; 14(3): 275–291. doi: 10.1016/j.jiec.2008.01.011
83. Cho YK, Park EJ, Kim YD. Removal of oil by gelation using hydrophobic silica nanoparticles. *Journal of Industrial and Engineering Chemistry* 2014; 20(4): 1231–1235. doi: 10.1016/j.jiec.2013.08.005
84. Nguyen ST, Feng J, Ng SK, et al. Advanced thermal insulation and absorption properties of recycled cellulose aerogels. *Colloids and Surfaces A: Physicochemical and Engineering Aspects* 2014; 445: 128–134. doi: 10.1016/j.colsurfa.2014.01.015
85. Salernitano E, Migliaresi C. Composite materials for biomedical applications: A review. *Journal of Applied Biomaterials & Biomechanics* 2003; 1(1): 3–18.
86. McInnes SJP, Irani Y, Williams KA, Voelcker NH. Controlled drug delivery from composites of nanostructured porous silicon and poly(L-lactide). *Nanomedicine* 2012; 7(7): 995–1016. doi: 10.2217/nnm.11.176
87. Rho W-Y, Kim H-M, Kyeong S, et al. Facile synthesis of monodispersed silica-coated magnetic nanoparticles. *Journal of Industrial and Engineering Chemistry* 2014; 20(5): 2646–2649. doi: 10.1016/j.jiec.2013.12.014
88. Wu H, Zhao Y, Mu X, et al. A silica–polymer composite nano system for tumor-targeted imaging and p53 gene therapy of lung cancer. *Journal of Biomaterials Science, Polymer Edition* 2015; 26(6): 384–400. doi: 10.1080/09205063.2015.1012035
89. Zhang T, Zhang L, Li C. Study of the preparation and properties of PBT/Epoxy/SiO_2 nanocomposites. *Journal of Macromolecular Science, Part B* 2011; 50(5): 967–974. doi: 10.1080/00222348.2010.497112
90. Liu H, Xu J, Guo B, He X. Preparation and performance of silica/polypropylene composite separator for lithium-ion batteries. *Journal of Materials Science* 2014; 49: 6961–6966. doi: 10.1007/s10853-014-8401-2
91. Raveh M, Liu L, Mandler D. Electrochemical co-deposition of conductive polymer–silica hybrid thin films. *Physical Chemistry Chemical Physics* 2013; 15(26): 10876–10884. doi: 10.1039/C3CP50457C
92. Lee DW, Yoo BR. Advanced silica/polymer composites: Materials and applications. *Journal of Industrial and Engineering Chemistry* 2016; 38: 1–12. doi: 10.1016/j.jiec.2016.04.016
93. Tong H, Chen H, Zhao Y, et al. Robust PDMS-based porous sponge with enhanced recyclability for selective separation of oil-water mixture. *Colloids and Surfaces A: Physicochemical and Engineering Aspects* 2022; 648: 129228. doi: 10.1016/j.colsurfa.2022.129228
94. Zhao X, Li L, Li B, et al. Durable superhydrophobic/superoleophilic PDMS sponges and their applications in selective oil absorption and in plugging oil leakages. *Journal of Materials Chemistry A* 2014; 2(43): 18281–18287. doi: 10.1039/C4TA04406A
95. Choi S-J, Kwon T-H, Im H, et al. A polydimethylsiloxane (PDMS) sponge for the selective absorption of oil from water. *ACS Applied Materials & Interfaces* 2011; 3(12): 4552–4556. doi: 10.1021/am201352w
96. Yu C, Yu C, Cui L, et al. Facile preparation of the porous PDMS oil-absorbent for oil/water separation. *Advanced Materials Interfaces* 2017; 4(3): 1600862. doi: 10.1002/admi.201600862
97. He X, Mu X, Wen Q, et al. Flexible and transparent triboelectric nanogenerator based on high performance well-ordered porous PDMS dielectric film. *Nano Research* 2016; 9: 3714–3724. doi: 10.1007/s12274-016-1242-3

98. Chen M, Zhang L, Duan S, et al. Highly stretchable conductors integrated with a conductive carbon nanotube/graphene network and 3D porous poly(dimethylsiloxane). *Advanced Functional Materials* 2014; 24(47): 7548–7556. doi: 10.1002/adfm.201401886
99. Lee KY, Chun J, Lee J-H, et al. Hydrophobic sponge structure-based triboelectric nanogenerator. *Advanced Materials* 2014; 26(29): 5037–5042. doi: 10.1002/adma.201401184
100. Wang J, Guo J, Si P, et al. Polydopamine-based synthesis of an $In(OH)_3$–PDMS sponge for ammonia detection by switching surface wettability. *RSC Advances* 2016; 6(6): 4329–4334. doi: 10.1039/C5RA23484K
101. Jiao K, Graham CL, Wolff J, et al. Modulating molecular and nanoparticle transport in flexible polydimethylsiloxane membranes. *Journal of Membrane Science* 2012; 401–402: 25–32. doi: 10.1016/j.memsci.2012.01.015
102. Li J, Zhang Y. Porous polymer films with size-tunable surface pores. *Chemistry of Materials* 2007; 19(10): 2581–2584. doi: 10.1021/cm070197v
103. Peng S, Hartley PG, Hughes TC, Guo Q. Controlling morphology and porosity of porous siloxane membranes through water content of precursor microemulsion. *Soft Matter* 2012; 8(40): 10493–10501. doi: 10.1039/C2SM26312B
104. Liang S, Li Y, Yang J, et al. 3D stretchable, compressible, and highly conductive metal-coated polydimethylsiloxane sponges. *Advanced Materials Technologies* 2006; 1(7): 1600117. doi: 10.1002/admt.201600117
105. Jung S, Kim JH, Kim J, et al. Reverse-micelle-induced porous pressure-sensitive rubber for wearable human–machine interfaces. *Advanced Materials* 2014; 26(28): 4825–4830. doi: 10.1002/adma.201401364
106. Giustiniani A, Guégan P, Marchand M, et al. Generation of silicone poly-HIPEs with controlled pore sizes via reactive emulsion stabilization. *Macromolecular Rapid Communications* 2016; 37(18): 1527–1532. doi: 10.1002/marc.201600281
107. Kovalenko A, Zimny K, Mascaro B, et al. Tailoring of the porous structure of soft emulsion-templated polymer materials. *Soft Matter* 2016; 12(23): 5154–5163. doi: 10.1039/C6SM00461J
108. Grosse MT, Lamotte M, Birot M, Deleuze H. Preparation of microcellular polysiloxane monoliths. *Journal of Polymer Science Part A: Polymer Chemistry* 2008; 46(1): 21–32. doi: 10.1002/pola.22351
109. Lee H, Yoo J-K, Park J-H, et al. A stretchable polymer–carbon nanotube composite electrode for flexible lithium-ion batteries: Porosity engineering by controlled phase separation. *Advanced Energy Materials* 2012; 2(8): 976–982. doi: 10.1002/aenm.201100725
110. Zhao J, Luo G, Wu J, Xia H. Preparation of microporous silicone rubber membrane with tunable pore size via solvent evaporation-induced phase separation. *ACS Applied Materials & Interfaces* 2013; 5(6): 2040–2046. doi: 10.1021/am302929c
111. Hinton TJ, Hudson A, Pusch K, et al. 3D printing PDMS elastomer in a hydrophilic support bath via freeform reversible embedding. *ACS Biomaterials Science & Engineering* 2016; 2(10): 1781–1786. doi: 10.1021/acsbiomaterials.6b00170
112. Kolesky DB, Homan KA, Skylar-Scott MA, Lewis JA. Three-dimensional bioprinting of thick vascularized tissues. *PNAS* 2016; 113(12): 3179–3184. doi: 10.1073/pnas.1521342113
113. Qin Z, Compton BG, Lewis JA, Buehler MJ. Structural optimization of 3D-printed synthetic spider webs for high strength. *Nature Communications* 2015; 6: 7038. doi: 10.1038/ncomms8038
114. Guo J, Wang J, Wang W, et al. The fabrication of 3D porous PDMS sponge for oil and organic solvent absorption. *Environmental Progress & Sustainable Energy* 2019; 38(S1): S86–S92. doi: 10.1002/ep.12924
115. Tan D, Fan W, Xiong W, et al. Study on adsorption performance of conjugated microporous polymers for hydrogen and organic solvents: The role of pore volume. *European Polymer Journal* 2012; 48(4): 705–711. doi: 10.1016/j.eurpolymj.2012.01.012
116. You L, Temiyasathit S, Tao E, et al. 3D microfluidic approach to mechanical stimulation of osteocyte processes. *Cellular and Molecular Bioengineering* 2008; 1: 103–107. doi: 10.1007/s12195-008-0010-1
117. Li N, Li T, Lei X, et al. Preparation and characterization of porous PDMS beads for oil and organic solvent sorption. *Polymer Engineering & Science* 2014; 54(12): 2965–2969. doi: 10.1002/pen.23860
118. Hayase G, Kanamori K, Hasegawa G, et al. A superamphiphobic macroporous silicone monolith with marshmallow-like flexibility. *Angewandte Chemie International Edition* 2013; 52(41): 10788–10791. doi: 10.1002/anie.201304169
119. Verdejo R, Barroso-Bujans F, Rodriguez-Perez MA, et al. Functionalized graphene sheet filled silicone foam nanocomposites. *Journal of Materials Chemistry* 2008; 18(19): 2221–2226. doi: 10.1039/B718289A
120. Li L, Li B, Wu L, et al. Magnetic, superhydrophobic and durable silicone sponges and their applications in removal of organic pollutants from water. *Chemical Communications* 2014; 50(58): 7831–7833. doi: 10.1039/C4CC03045A
121. Moitra N, Kanamori K, Shimada T, et al. Synthesis of hierarchically porous hydrogen silsesquioxane monoliths and embedding of metal nanoparticles by on-site reduction. *Advanced Functional Materials* 2013; 23(21): 2714–2722. doi: 10.1002/adfm.201202558
122. Si P, Wang J, Zhao C, et al. Preparation and morphology control of three-dimensional interconnected microporous PDMS for oil sorption. *Polymers for Advanced Technologies* 2015; 26(9): 1091–1096. doi: 10.1002/pat.3538

123. Wang C-F, Lin S-J. Robust superhydrophobic/superoleophilic sponge for effective continuous absorption and expulsion of oil pollutants from water. ACS Applied Materials & Interfaces 2013; 5(18): 8861–8864. doi: 10.1021/am403266v
124. Jiang G, Hu R, Xi X, et al. Facile preparation of superhydrophobic and superoleophilic sponge for fast removal of oils from water surface. *Journal of Materials Research* 2013; 28: 651–656. doi: 10.1557/jmr.2012.410
125. Krishnan M, Michal F, Alsoughayer S, et al. Thermodynamic and kinetic investigation of water absorption by PAM composite hydrogel. In: SPE Kuwait Oil & Gas Show and Conference; 13–16 October 2019; Mishref, Kuwait. doi: 10.2118/198033-MS
126. Almohsin A, Krishnan MR, Alsharaeh E, Harbi B. Preparation and properties investigation on sand-polyacrylamide composites with engineered interfaces for water shutoff applications. In: Middle East Oil, Gas and Geosciences Show; 19–21 February 2023; Manama, Bahrain. doi: 10.2118/213481-MS
127. Almohsin A, Michal F, Alsharaeh E, et al. Self-healing PAM composite hydrogel for water shutoff at high temperatures: Thermal and rheological investigations. In: SPE Gas & Oil Technology Showcase and Conference; 21–23 October 2019; Dubai, UAE. doi: 10.2118/198664-MS
128. Almohsin A, Alsharaeh E, Michael FM, Krishnan MR. Polymer-Nanofiller Hydrogels. U.S. Patent US20,220,290,033A1, 15 September 2022.
129. Almohsin A, Alsharaeh E, Krishnan MR, Alghazali M. Coated Nanosand as Relative Permeability Modifier. U.S. Patent US11,499,092B2, 15 November 2022.
130. Keishnan MR, Michael FM, Almohsin AM, Alsharaeh EH. Thermal and rheological investigations on N,N'-methylenebis acrylamide cross-linked polyacrylamide nanocomposite hydrogels for water shutoff applications. In: Offshore Technology Conference Asia; 2–6 November 2020; Kuala Lumpur, Malaysia. doi: 10.4043/30123-MS
131. Michael FM, Krishnan MR, Fathima A, et al. Zirconia/graphene nanocomposites effect on the enhancement of thermo-mechanical stability of polymer hydrogels. *Materials Today Communications* 2019; 21: 100701. doi: 10.1016/j.mtcomm.2019.100701
132. Michael FM, Krishnan MR, AlSoughayer S, et al. Thermo-elastic and self-healing polyacrylamide -2D nanofiller composite hydrogels for water shutoff treatment. *Journal of Petroleum Science and Engineering* 2020; 193: 107391. doi: 10.1016/j.petrol.2020.107391
133. Lee SG, Ham DS, Lee DY, et al. Transparent superhydrophobic/translucent superamphiphobic coatings based on silica–fluoropolymer hybrid nanoparticles. *Langmuir* 2013; 29(48): 15051–15057. doi: 10.1021/la404005b
134. Sriram S, Kumar A. Separation of oil-water via porous PMMA/SiO_2 nanoparticles superhydrophobic surface. *Colloids and Surfaces A: Physicochemical and Engineering Aspects* 2019; 563: 271–279. doi: 10.1016/j.colsurfa.2018.12.017
135. Zhong M, Zhang Y, Li X, Wu X. Facile fabrication of durable superhydrophobic silica/epoxy resin coatings with compatible transparency and stability. *Surface and Coatings Technology* 2018; 347: 191–198. doi: 10.1016/j.surfcoat.2018.04.063
136. Ebert D, Bhushan B. Transparent, superhydrophobic, and wear-resistant coatings on glass and polymer substrates using SiO_2, ZnO, and ITO nanoparticles. *Langmuir* 2012; 28(31): 11391–11399. doi: 10.1021/la301479c
137. Manoudis P, Papadopoulou S, Karapanagiotis I, et al. Polymer-silica nanoparticles composite films as protective coatings for stone-based monuments. *Journal of Physics: Conference Series* 2007; 61: 1361. doi: 10.1088/1742-6596/61/1/269
138. Krishnan MR, Aldawsari Y, Michael FM, et al. Mechanically reinforced polystyrene-polymethyl methacrylate copolymer-graphene and Epoxy-Graphene composites dual-coated sand proppants for hydraulic fracture operations. *Journal of Petroleum Science and Engineering* 2021; 196: 107744. doi: 10.1016/j.petrol.2020.107744
139. Krishnan MR, Michael FM, Almohsin A, Alsharaeh EH. Polyacrylamide hydrogels coated super-hydrophilic sand for enhanced water storage and extended release. *SSRN* 2022.
140. Krishnan MR, Aldawsari Y, Michael FM, et al. 3D-Polystyrene-polymethyl methacrylate/divinyl benzene networks-Epoxy-Graphene nanocomposites dual-coated sand as high strength proppants for hydraulic fracture operations. J*ournal of Natural Gas Science and Engineering* 2021; 88: 103790. doi: 10.1016/j.jngse.2020.103790
141. Krishnan MR, Omar H, Aldawsari Y, et al. Insight into thermo-mechanical enhancement of polymer nanocomposites coated microsand proppants for hydraulic fracturing. *Heliyon* 2022; 8(12): e12282. doi: 10.1016/j.heliyon.2022.e12282
142. Krishnan MR, Li W, Alsharaeh EH. Ultra-lightweight nanosand/polymer nanocomposite materials for hydraulic fracturing operations. *Polymer Nanocomposite Materials for Hydraulic Fracturing Operations* 2022.
143. Krishnan MR, Omar H, Almohsin A, Alsharaeh EH. An overview on nanosilica–polymer composites as high-performance functional materials in oil fields. *Polymer Bulletin* 2023. doi: 10.1007/s00289-023-04934-y
144. 68. Li W, Alsharaeh E, Krishnan MR. Coated Proppant and Methods of Making and Use Thereof. U.S. Patent 20,230,313,027A1, 5 October 2023.
145. 70. Li W, Alsharaeh E, Krishnan MR. Methods for Making Proppant Coatings. U.S. Patent 11,459,503, 4 October 2022.
146. Michael FM, Krishnan MR, Li W, Alsharaeh EH. A review on polymer-nanofiller composites in developing coated sand proppants for hydraulic fracturing. *Journal of Natural Gas Science and Engineering* 2020; 83: 103553. doi: 10.1016/j.jngse.2020.103553

147. Fielding LA, Tonnar J, Armes SP. All-acrylic film-forming colloidal polymer/silica nanocomposite particles prepared by aqueous emulsion polymerization. *Langmuir* 2011; 27(17): 11129–11144. doi: 10.1021/la202066n
148. Zhou C, Xu S, Pi P, et al. Polyacrylate/silica nanoparticles hybrid emulsion coating with high silica content for high hardness and dry-wear-resistant. *Progress in Organic Coatings* 2018; 121: 30–37. doi: 10.1016/j.porgcoat.2018.04.001
149. Zhang S-W, Zhou S-X, Weng Y-M, Wu L-M. Synthesis of SiO_2/polystyrene nanocomposite particles via miniemulsion polymerization. *Langmuir* 2005; 21(6): 2124–2128. doi: 10.1021/la047652b
150. Monteil V, Stumbaum J, Thomann R, Mecking S. Silica/polyethylene nanocomposite particles from catalytic emulsion polymerization. *Macromolecules* 2006; 39(6): 2056–2062. doi: 10.1021/ma052737k
151. Kim D, Lee JS, Barry CMF, Mead JL. Effect of fill factor and validation of characterizing the degree of mixing in polymer nanocomposites. *Polymer Engineering and Science* 2007; 47(12): 2049–2056. doi: 10.1002/pen.20920
152. Mittal V (editor). *Synthesis Techniques for Polymer Nanocomposites*. Wiley-VCH Verlag GmbH & Co. KGaA; 2015. doi: 10.1002/9783527670307
153. Yang F, Nelson GL. PMMA/silica nanocomposite studies: Synthesis and properties. *Journal of Applied Polymer Science* 2004; 91(6): 3844–3850. doi: 10.1002/app.13573
154. Ou C-F, Hsu M-C. Preparation and characterization of cyclo olefin copolymer (COC)/silica nanoparticle composites by solution blending. *Journal of Polymer Research* 2007; 14: 373–378. doi: 10.1007/s10965-007-9119-5
155. Huang J-W, Wen Y-L, Kang C-C, Yeh M-Y. Preparation of polyimide-silica nanocomposites from nanoscale colloidal silica. *Polymer Journal* 2007; 39(7): 654–658.
156. Stöber W, Fink A, Bohn E. Controlled growth of monodisperse silica spheres in the micron size range. *Journal of Colloid and Interface Science* 1968; 26(1): 62–69. doi: 10.1016/0021-9797(68)90272-5
157. Shang X, Zhu Z, Yin J, Ma X. Compatibility of soluble polyimide/silica hybrids induced by a coupling agent. *Chemistry of Materials* 2002; 14(1): 71–77. doi: 10.1021/cm010088v
158. Zhang S, Yu A, Song X, Liu S. Synthesis and characterization of waterborne UV-curable polyurethane nanocomposites based on the macromonomer surface modification of colloidal silica. *Progress in Organic Coatings* 2013; 76(7–8): 1032–1039. doi: 10.1016/j.porgcoat.2013.02.019
159. Zhang Y-L, Xia H, Kim E, Sun H-B. Recent developments in superhydrophobic surfaces with unique structural and functional properties. *Soft Matter* 2012; 8(44): 11217–11231. doi: 10.1039/C2SM26517F
160. Liu M, Zheng Y, Zhai J, Jiang L. Bioinspired super-antiwetting interfaces with special liquid−solid adhesion. *Accounts of Chemical Research* 2010; 43(3): 368–377. doi: 10.1021/ar900205g
161. Li Y, Lee EJ, Cho SO. Superhydrophobic coatings on curved surfaces featuring remarkable supporting force. *The Journal of Physical Chemistry C* 2007; 111(40): 14813–14817. doi: 10.1021/jp0736721
162. Voronov RS, Papavassiliou DV, Lee LL. Review of fluid slip over superhydrophobic surfaces and its dependence on the contact angle. *Industrial & Engineering Chemistry Research* 2008; 47(8): 2455–2477. doi: 10.1021/ie0712941
163. Koc Y, de Mello AJ, McHale G, et al. Nano-scale superhydrophobicity: suppression of protein adsorption and promotion of flow-induced detachment. *Lab on a Chip* 2008; 8(4): 582–586. doi: 10.1039/B716509A
164. Feng L, Li S, Li Y, et al. Super-hydrophobic surfaces: From natural to artificial. *Advanced Materials* 2002; 14(24): 1857–1860. doi: 10.1002/adma.200290020
165. Cao L, Jones AK, Sikka VK, et al. Anti-icing superhydrophobic coatings. *Langmuir* 2009; 25(21): 12444–12448. doi: 10.1021/la902882b
166. Kulinich SA, Farzaneh M. How wetting hysteresis influences ice adhesion strength on superhydrophobic surfaces. *Langmuir* 2009; 25(16): 8854–8856. doi: 10.1021/la901439c
167. Wu D, Wu S-Z, Chen Q-D, et al. Curvature-driven reversible in situ switching between pinned and roll-down superhydrophobic states for water droplet transportation. *Advanced Materials* 2011; 23(4): 545–549. doi: 10.1002/adma.201001688
168. Wang M, Chen C, Ma J, Xu J. Preparation of superhydrophobic cauliflower-like silica nanospheres with tunable water adhesion. *Journal of Materials Chemistry* 2011; 21(19): 6962–6967. doi: 10.1039/C1JM10283D
169. Bravo J, Zhai L, Wu Z, et al. Transparent superhydrophobic films based on silica nanoparticles. *Langmuir* 2007; 23(13): 7293–7298. doi: 10.1021/la070159q
170. Ming W, Wu D, van Benthem R, de With G. Superhydrophobic films from raspberry-like particles. *Nano Letters* 2005; 5(11): 2298–2301. doi: 10.1021/nl0517363
171. Yang S, Wang L, Wang C-F, et al. Superhydrophobic thermoplastic polyurethane films with transparent/fluorescent performance. *Langmuir* 2010; 26(23): 18454–18458. doi: 10.1021/la103496t
172. Tang X, Wang T, Yu F, et al. Simple, robust and large-scale fabrication of superhydrophobic surfaces based on silica/polymer composites. *RSC Advances* 2013; 3(48): 25670–25673. doi: 10.1039/C3RA44502J
173. Wang S-D, Shu Y-Y. Superhydrophobic antireflective coating with high transmittance. *Journal of Coatings Technology and Research* 2013; 10: 527–535. doi: 10.1007/s11998-012-9468-9
174. Xu Y, Wu D, Sun YH, et al. Comparative study on hydrophobic anti-reflective films from three kinds of methyl-modified silica sols. *Journal of Non-Crystalline Solids* 2005; 351(3): 258–266. doi: 10.1016/j.jnoncrysol.2004.11.011

175. Chang K-C, Chen Y-K, Chen H. Fabrication of highly transparent and superhydrophobic silica-based surface by TEOS/PPG hybrid with adjustment of the pH value. *Surface and Coatings Technology* 2008; 202(16): 3822–3831. doi: 10.1016/j.surfcoat.2008.01.028
176. Krishnan M, Chen H-Y, Ho R-M. Switchable structural colors from mesoporous polystyrene films. In: ACS 252nd National Meeting; 18–26 August 2016; Philadelphia.
177. Krishnan MR, Rajendran V, Alsharaeh E. Anti-reflective and high-transmittance optical films based on nanoporous silicon dioxide fabricated from templated synthesis. *Journal of Non-Crystalline Solids* 2023; 606: 122198. doi: 10.1016/j.jnoncrysol.2023.122198
178. Lin T-X, Hsu F-M, Lee Y-L, et al. Biomimetic synthesis of antireflective silica/polymer composite coatings comprising vesicular nanostructures. *ACS Applied Materials & Interfaces* 2016; 8(39): 26309–26318. doi: 10.1021/acsami.6b07874
179. Xu L, He J. Antifogging and antireflection coatings fabricated by integrating solid and mesoporous silica nanoparticles without any post-treatments. *ACS Applied Materials & Interfaces* 2012; 4(6): 3293–3299. doi: 10.1021/am300658e
180. Hammer P, dos Santos FC, Cerrutti BM, et al. Highly corrosion resistant siloxane-polymethyl methacrylate hybrid coatings. *Journal of Sol-Gel Science and Technology* 2012; 63: 266–274. doi: 10.1007/s10971-011-2672-8
181. dos Santos FC, Harb SV, Menu M-J, et al. On the structure of high performance anticorrosive PMMA–siloxane–silica hybrid coatings. *RSC Advances* 2015; 5(129): 106754–106763. doi: 10.1039/C5RA20885H
182. Sarmento VHV, Schiavetto MG, Hammer P, et al. Corrosion protection of stainless steel by polysiloxane hybrid coatings prepared using the sol–gel process. *Surface and Coatings Technology* 2010; 204(16–17): 2689–2701. doi: 10.1016/j.surfcoat.2010.02.022
183. Mishra AK, Bose S, Kuila T, et al. Silicate-based polymer-nanocomposite membranes for polymer electrolyte membrane fuel cells. *Progress in Polymer Science* 2012; 37(6): 842–869. doi: 10.1016/j.progpolymsci.2011.11.002
184. Bae I, Oh K-H, Yun S-H, Kim H. Asymmetric silica composite polymer electrolyte membrane for water management of fuel cells. *Journal of Membrane Science* 2017; 542: 52–59. doi: 10.1016/j.memsci.2017.07.058
185. Sambandam S, Ramani V. SPEEK/functionalized silica composite membranes for polymer electrolyte fuel cells. *Journal of Power Sources* 2007; 170(2): 259–267. doi: 10.1016/j.jpowsour.2007.04.026
186. Wen S, Gong C, Tsen W-C, et al. Sulfonated poly(ether sulfone)/silica composite membranes for direct methanol fuel cells. *Journal of Applied Polymer Science* 2010; 116(3): 1491–1498. doi: 10.1002/app.31699
187. Shaari N, Kamarudin SK. Recent advances in additive-enhanced polymer electrolyte membrane properties in fuel cell applications: An overview. *International Journal of Energy Research* 2019; 43(7): 2756–2794. doi: 10.1002/er.4348
188. Lee C, Na H, Jeon Y, et al. Poly(ether imide) nanofibrous web composite membrane with SiO_2/heteropolyacid ionomer for durable and high-temperature polymer electrolyte membrane (PEM) fuel cells. *Journal of Industrial and Engineering Chemistry* 2019; 74: 7–13. doi: 10.1016/j.jiec.2019.01.034
189. Tripathi BP, Shahi VK. Organic–inorganic nanocomposite polymer electrolyte membranes for fuel cell applications. *Progress in Polymer Science* 2011; 36(7): 945–979. doi: 10.1016/j.progpolymsci.2010.12.005
190. Chen C-Y, Garnica-Rodriguez JI, Duke MC, et al. Nafion/polyaniline/silica composite membranes for direct methanol fuel cell application. *Journal of Power Sources* 2007; 166(2): 324–330. doi: 10.1016/j.jpowsour.2006.12.102
191. Su Y-H, Liu Y-L, Sun Y-M, et al. Using silica nanoparticles for modifying sulfonated poly(phthalazinone ether ketone) membrane for direct methanol fuel cell: A significant improvement on cell performance. *Journal of Power Sources* 2006; 155(2): 111–117. doi: 10.1016/j.jpowsour.2005.03.233
192. Antonucci PL, Aricò AS, Cretì P, et al. Investigation of a direct methanol fuel cell based on a composite Nafion®-silica electrolyte for high temperature operation. *Solid State Ionics* 1999; 125(1–4): 431–437. doi: 10.1016/S0167-2738(99)00206-4
193. Saxena A, Tripathi BP, Shahi VK. Sulfonated poly(styrene-*co*-maleic anhydride)−poly(ethylene glycol)−silica nanocomposite polyelectrolyte membranes for fuel cell applications. *The Journal of Physical Chemistry B* 2007; 111(43): 12454–12461. doi: 10.1021/jp072244c
194. Kanamura K, Mitsui T, Munakata H. Preparation of composite membrane between a uniform porous silica matrix and injected proton conductive gel polymer. *Chemistry of Materials* 2005; 17(19): 4845–4851. doi: 10.1021/cm047979y
195. Wang Y-Y, Hsieh T-E. Effect of UV curing on electrical properties of a UV-curable co-polyacrylate/silica nanocomposite as a transparent encapsulation resin for device packaging. *Macromolecular Chemistry and Physics* 2007; 208(22): 2396–2402. doi: 10.1002/macp.200700229
196. Wijesiri RP, Knowles GP, Yeasmin H, et al. CO_2 capture from air using pelletized polyethylenimine impregnated MCF silica. *Industrial & Engineering Chemistry Research* 2019; 58(8): 3293–3303. doi: 10.1021/acs.iecr.8b04973
197. Chaikittisilp W, Khunsupat R, Chen TT, Jones CW. Poly(allylamine)–mesoporous silica composite materials for CO_2 capture from simulated flue gas or ambient air. *Industrial & Engineering Chemistry Research* 2011; 50(24): 14203–14210. doi: 10.1021/ie201584t

198. Holewinski A, Sakwa-Novak MA, Carrillo J-MY, et al. Aminopolymer mobility and support interactions in silica-PEI composites for CO_2 capture applications: A quasielastic neutron scattering study. *The Journal of Physical Chemistry B* 2017; 121(27): 6721–6731. doi: 10.1021/acs.jpcb.7b04106
199. Sujan AR, Pang SH, Zhu G, et al. Direct CO_2 capture from air using poly(ethylenimine)-loaded polymer/silica fiber sorbents. *ACS Sustainable Chemistry & Engineering* 2019; 7(5): 5264–5273. doi: 10.1021/acssuschemeng.8b06203
200. Rezaei F, Lively RP, Labreche Y, et al. Aminosilane-grafted polymer/silica hollow fiber adsorbents for CO_2 capture from flue gas. *ACS Applied Materials & Interfaces* 2013; 5(9): 3921–3931. doi: 10.1021/am400636c
201. Lu X, Manners I, Winnik MA. Polymer/silica composite films as luminescent oxygen sensors. *Macromolecules* 2001; 34(6): 1917–1927. doi: 10.1021/ma001454j
202. Timin AS, Solomonov AV, Kumagai A, et al. Magnetic polymer-silica composites as bioluminescent sensors for bilirubin detection. *Materials Chemistry and Physics* 2016; 183: 422–429. doi: 10.1016/j.matchemphys.2016.08.048
203. Comes M, Dolores Marcos M, Martínez-Máñez R, et al. Hybrid functionalised mesoporous silica–polymer composites for enhanced analyte monitoring using optical sensors. *Journal of Materials Chemistry* 2008; 18(47): 5815–5823. doi: 10.1039/B810992C
204. Shi Y, Seliskar CJ. Optically transparent polyelectrolyte−silica composite materials: Preparation, characterization, and application in optical chemical sensing. *Chemistry of Materials* 1997; 9(3): 821–829. doi: 10.1021/cm960495k
205. Rastogi PK, Ganesan V, Krishnamoorthi S. Palladium nanoparticles incorporated polymer-silica nanocomposite based electrochemical sensing platform for nitrobenzene detection. *Electrochimica Acta* 2014; 147: 442–450. doi: 10.1016/j.electacta.2014.09.128
206. Liang F, Sayed M, Al-Muntasheri GA, et al. A comprehensive review on proppant technologies. *Petroleum* 2016; 2(1): 26–39. doi: 10.1016/j.petlm.2015.11.001
207. Zoveidavianpoor M, Gharibi A. Application of polymers for coating of proppant in hydraulic fracturing of subterraneous formations: A comprehensive review. *Journal of Natural Gas Science and Engineering* 2015; 24: 197–209. doi: 10.1016/j.jngse.2015.03.024
208. Nguyen PD, Dusterhoft RG, Dewprashad BT, Weaver JD. New guidelines for applying curable resin-coated proppants. In: SPE Formation Damage Control Conference; 18–19 February 1998; Lafayette, Louisiana. doi: 10.2118/39582-MS
209. Nguyen PD, Weaver JD, Desai BD. Methods of Coating Resin and Blending Resin-Coated Proppant. U.S. Patent 20,040,221,992A1, 11 November 2004.
210. Dewprashad B, Abass H, Meadows DL, et al. A method to select resin-coated proppants. In: SPE Annual Technical Conference and Exhibition; 3–6 October 1993; Houston, Texas. doi: 10.2118/26523-MS
211. Hussain H, McDaniel RR, Callanan MJ. Proppants with Fiber Reinforced Resin Coatings. U.S. Patent 6,528,157, 4 March 2003.
212. Stevens B. Fracking what makes it tick: Demystifying the Why's, technology and science behind unconventional oil and shale gas extraction behind unconventional oil and shale gas extraction. Presented at Fracking What Makes it Tick?–Demystifying the Why's, Technology and Science; 23 September 2014; Online.
213. Men X, Ge B, Li P, et al. Facile fabrication of superhydrophobic sand: Potential advantages for practical application in oil–water separation. *Journal of the Taiwan Institute of Chemical Engineers* 2016; 60: 651–655. doi: 10.1016/j.jtice.2015.11.015
214. Chen L, Wu Y, Guo Z. Superhydrophobic sand grains structured with aligned $Cu(OH)_2$ nano-needles for efficient oily water treatment. *Materials & Design* 2017; 135: 377–384. doi: 10.1016/j.matdes.2017.09.047
215. Liu P, Niu L, Tao X, et al. Preparation of superhydrophobic-oleophilic quartz sand filter and its application in oil-water separation. *Applied Surface Science* 2018; 447: 656–663. doi: 10.1016/j.apsusc.2018.04.030
216. Atta AM, Abdullah M, Al-Lohedan HA, Mohamed NH. Coating sand with new hydrophobic and superhydrophobic silica/paraffin wax nanocapsules for desert water storage and transportation. *Coatings* 2019; 9(2): 124. doi: 10.3390/coatings9020124
217. Montesano FF, Parente A, Santamaria P, et al. Biodegradable superabsorbent hydrogel increases water retention properties of growing media and plant growth. *Agriculture and Agricultural Science Procedia* 2015; 4: 451–458. doi: 10.1016/j.aaspro.2015.03.052
218. Khodadadi Dehkordi D. Effect of superabsorbent polymer on soil and plants on steep surfaces. *Water and Environment Journal* 2018; 32(2): 158–163. doi: 10.1111/wej.12309
219. Liao R, Wu W, Ren S, Yang P. Effects of superabsorbent polymers on the hydraulic parameters and water retention properties of soil. *Journal of Nanomaterials* 2016; 2016: 5403976. doi: 10.1155/2016/5403976
220. Chen L, Si Y, Guo Z, Liu W. Superhydrophobic sand: A hope for desert water storage and transportation projects. *Journal of Materials Chemistry A* 2017; 5(14): 6416–6423. doi: 10.1039/C7TA00962C
221. Sivasubramanian M, Nedunjezhian K, Murugesan S, Kalpoondi Sekar R. Sub-micron dispersions of sand in water prepared by stirred bead milling and ultrasonication: A potential coolant. *Applied Thermal Engineering* 2012; 44: 1–10. doi: 10.1016/j.applthermaleng.2012.04.004

222. Manikandan S, Shylaja A, Rajan KS. Thermo-physical properties of engineered dispersions of nano-sand in propylene glycol. *Colloids and Surfaces A: Physicochemical and Engineering Aspects* 2014; 449: 8–18. doi: 10.1016/j.colsurfa.2014.02.040
223. Phuong N, Andisetiawan A, Van Lam D, et al. Nano sand filter with functionalized nanoparticles embedded in anodic aluminum oxide templates. *Scientific Reports* 2016; 6: 37673. doi: 10.1038/srep37673
224. Zheng Y, Chonung K, Wang G, et al. Epoxy/nano-silica composites: Curing kinetics, glass transition temperatures, dielectric, and thermal–mechanical performances. *Journal of Applied Polymer Science* 2009; 111(2): 917–927. doi: 10.1002/app.28875
225. Ahmad T, Mamat O, Ahmad R. Studying the effects of adding silica sand nanoparticles on epoxy based composites. *Journal of Nanoparticles* 2013; 2013: 603069. doi: 10.1155/2013/603069
226. Rizlan Z, Mamat O. Mechanical milling of Tronoh silica sand nanoparticles using low speed ball milling process. *Applied Mechanics and Materials* 2014; 465–466: 998–1002. doi: 10.4028/www.scientific.net/AMM.465-466.998
227. Ahmad T, Mamat O. Tronoh silica sand nanoparticle production and applications design for composites. *Defect and Diffusion Forum* 2012; 330: 39–47. doi: 10.4028/www.scientific.net/DDF.330.39
228. Ahmad T, Ahmad R, Kamran M, et al. Effect of Thal silica sand nanoparticles and glass fiber reinforcements on epoxy-based hybrid composite. *Iranian Polymer Journal* 2015; 24: 21–27. doi: 10.1007/s13726-014-0296-x
229. Sui G, Jana S, Salehi-khojin A, et al. Preparation and properties of natural sand particles reinforced epoxy composites. *Macromolecular Materials and Engineering* 2007; 292(4): 467–473. doi: 10.1002/mame.200600479
230. Ahmed T, Mamat O. The development and properties of polypropylene-silica sand nanoparticles composites. In: 2011 IEEE Colloquium on Humanities, Science and Engineering; 5–6 December 2011; Penang, Malaysia. pp. 172–177. doi: 10.1109/CHUSER.2011.6163710
231. Schneider J. Nanostructured Sand, Process for Producing Nano Structured Sand, Process for Separating a Pollutant-Water Mixture with the Nanostructured Sand and Further Uses. U.S. Patent 20,170,065,961, 26 February 2019.
232. Krishnan MR, Alsharaeh E. Potential removal of benzene-toluene-xylene toxic vapors by nanoporous poly(styrene-*r*-methylmethacrylate) copolymer composites. *Environmental Nanotechnology, Monitoring & Management* 2023; 20: 100860. doi: 10.1016/j.enmm.2023.100860.
233. Krishnan MR, Chien Y-C, Cheng C-F, Ho R-M. Fabrication of mesoporous polystyrene films with controlled porosity and pore size by solvent annealing for templated syntheses. *Langmuir* 2017; 33(34): 8428–8435. doi: 10.1021/acs.langmuir.7b02195
234. Krishnan MR, Lu K-Y, Chiu W-Y, et al. Directed self-assembly of star-block copolymers by topographic nanopatterns through nucleation and growth mechanism. *Small* 2018; 14(16): 1704005. doi: 10.1002/smll.201704005
235. Lo T-Y, Krishnan MR, Lu K-Y, Ho R-M. Silicon-containing block copolymers for lithographic applications. *Progress in Polymer Science* 2018; 77: 19–68. doi: 10.1016/j.progpolymsci.2017.10.002
236. Alsharaeh EH, Othman AA. Microwave irradiation synthesis and characterization of RGO-AgNPs/polystyrene nanocomposites. *Polymer Composites* 2014; 35(12): 2318–2323. doi: 10.1002/pc.22896
237. Bongu CS, Krishnan MR, Soliman A, et al. Flexible and freestanding MoS_2/graphene composite for high-performance supercapacitors. *ACS Omega* 2023; 8(40): 36789–36800. doi: 10.1021/acsomega.3c03370
238. Cheng C-F, Chen Y-M, Zou F, et al. Li-ion capacitor integrated with nano-network-structured Ni/NiO/C anode and nitrogen-doped carbonized metal–organic framework cathode with high power and long cyclability. *ACS Applied Materials & Interfaces* 2019; 11(34): 30694–30702. doi: 10.1021/acsami.9b06354
239. Chien Y-C, Huang L-Y, Yang K-C, et al. Fabrication of metallic nanonetworks via templated electroless plating as hydrogenation catalyst. *Emergent Materials* 2021; 4: 493–501. doi: 10.1007/s42247-020-00108-y